9. Walker, L. M., Phogat, S. K., Chan-Hui, P. Y., Wagner, D., Phung, P., Goss, J. L., Wrin, T., Simek, M. D., Fling, S., Mitcham, J. L., Lehrman, J. K., Priddy, F. H., Olsen, O. A., Frey, S. M., Hammond, P. W.; Protocol G Principal Investigators, Kaminsky, S., Zamb, T., Moyle, M., Koff, W. C., Poignard, P., and Burton, D. R. (2009) Broad and potent neutralizing antibodies from an African donor reveal a new HIV-1 vaccine target. *Science* **326**, 285–289
10. Wu, X., Yang, Z. Y., Li, Y., Hogerkorp, C. M., Schief, W. R., Seaman, M. S., Zhou, T., Schmidt, S. D., Wu, L., Xu, L., Longo, N. S., McKee, K., O'Dell, S., Louder, M. K., Wycuff, D. L., Feng, Y., Nason, M., Doria-Rose, N., Connors, M., Kwong, P. D., Roederer, M., Wyatt, R. T., Nabel, G. J., and Mascola, J. R. (2010) Rational design of envelope identifies broadly neutralizing human monoclonal antibodies to HIV-1. *Science* **329**, 856–861
11. Walker, L. M., Huber, M., Doores, K. J., Falkowska, E., Pejchal, R., Julien, J. P., Wang, S. K., Ramos, A., Chan-Hui, P. Y., Moyle, M., Mitcham, J. L., Hammond, P. W., Olsen, O. A., Phung, P., Fling, S., Wong, C. H., Phogat, S., Wrin, T., Simek, M. D., Protocol G Principal Investigators, Koff, W. C., Wilson, I. A., Burton, D. R., and Poignard, P. (2011) Broad neutralization coverage of HIV by multiple highly potent antibodies. *Nature* **477**, 466–470
12. Scheid, J. F., Mouquet, H., Ueberheide, B., Diskin, R., Klein, F., Oliveira, T. Y., Pietzsch, J., Fenyo, D., Abadir, A., Velinzon, K., Hurley, A., Myung, S., Boulad, F., Poignard, P., Burton, D. R., Pereyra, F., Ho, D. D., Walker, B. D., Seaman, M. S., Bjorkman, P. J., Chait, B. T., and Nussenzweig, M. C. (2011) Sequence and structural convergence of broad and potent HIV antibodies that mimic CD4 binding. *Science* **333**, 1633–1637
13. Huang, J., Ofek, G., Laub, L., Louder, M. K., Doria-Rose, N. A., Longo, N. S., Imamichi, H., Bailer, R. T., Chakrabarti, B., Sharma, S. K., Alam, S. M., Wang, T., Yang, Y., Zhang, B., Migueles, S. A., Wyatt, R., Haynes, B. F., Kwong, P. D., Mascola, J. R., and Connors, M. (2012) Broad and potent neutralization of HIV-1 by a gp41-specific human antibody. *Nature* **491**, 406–412
14. Checkley, M. A., Luttge, B. G., and Freed, E. O. (2011) HIV-1 envelope glycoprotein biosynthesis, trafficking, and incorporation. *J. Mol. Biol.* **410**, 582–608
15. Berger, E. A., Murphy, P. M., and Farber, J. M. (1999) Chemokine receptors as HIV-1 coreceptors: roles in viral entry, tropism, and disease. *Annu. Rev. Immunol.* **17**, 657–700
16. Javaherian, K., Langlois, A. J., McDanal, C., Ross, K. L., Eckler, L. I., Jellis, C. L., Profy, A. T., Rusche, J. R., Bolognesi, D. P., Putney, S. D., et al. (1989) Principal neutralizing domain of the human immunodeficiency virus type 1 envelope protein. *Proc. Natl. Acad. Sci. USA* **86**, 6768–6772
17. Matsushita, S., Robert-Guroff, M., Rusche, J., Koito, A., Hattori, T., Hoshino, H., Javaherian, K., Takatsuki, K., and Putney, S. (1988) Characterization of a human immunodeficiency virus neutralizing monoclonal antibody and mapping of the neutralizing epitope. *J. Virol.* **62**, 2107–2114
18. Rusche, J. R., Javaherian, K., McDanal, C., Petro, J., Lynn, D. L., Grimaila, R., Langlois, A., Gallo, R. C., Arthur, L. O., Fischinger, P. J., et al. (1988) Antibodies that inhibit fusion of human immunodeficiency virus-infected cells bind a 24-amino acid sequence of the viral envelope, gp120. *Proc. Natl. Acad. Sci. USA* **85**, 3198–3202
19. Lynch, R. M., Shen, T., Gnanakaran, S., and Derdeyn, C. A. (2009) Appreciating HIV type 1 diversity: subtype differences in Env. *AIDS Res. Hum. Retroviruses* **25**, 237–248
20. Gorny, M. K., Williams, C., Volsky, B., Revesz, K., Cohen, S., Polonis, V. R., Honnen, W. J., Kayman, S. C., Krachmarov, C., Pinter, A., and Zolla-Pazner, S. (2002) Human monoclonal antibodies specific for conformation-sensitive epitopes of V3 neutralize human immunodeficiency virus type 1 primary isolates from various clades. *J. Virol.* **76**, 9035–9045
21. Pantophlet, R., Aguilar-Sino, R. O., Wrin, T., Cavacini, L. A., and Burton, D. R. (2007) Analysis of the neutralization breadth of the anti-V3 antibody F425-B4e8 and re-assessment of its epitope fine specificity by scanning mutagenesis. *Virology* **364**, 441–453
22. Hioe, C. E., Wrin, T., Seaman, M. S., Yu, X., Wood, B., Self, S., Williams, C., Gorny, M. K., and Zolla-Pazner, S. (2010) Anti-V3 monoclonal antibodies display broad neutralizing activities against multiple HIV-1 subtypes. *PLoS ONE* **5**, e10254
23. Conley, A. J., Gorny, M. K., Kessler II, J. A., Boots, L. J., Ossorio-Castro, M., Koenig, S., Lineberger, D. W., Emini, E. A., Williams, C., and Zolla-Pazner, S. (1994) Neutralization of primary human immunodeficiency virus type 1 isolates by the broadly reactive anti-V3 monoclonal antibody, 447-52D. *J. Virol.* **68**, 6994–7000
24. Gorny, M. K., Conley, A. J., Karwowska, S., Buchbinder, A., Xu, J. Y., Emini, E. A., Koenig, S., and Zolla-Pazner, S. (1992) Neutralization of diverse human immunodeficiency virus type 1 variants by an anti-V3 human monoclonal antibody. *J. Virol.* **66**, 7538–7542
25. Gorny, M. K., Williams, C., Volsky, B., Revesz, K., Wang, X. H., Burda, S., Kimura, T., Konings, F. A., Nádas, A., Anyangwe, C. A., Nyambi, P., Krachmarov, C., Pinter, A., and Zolla-Pazner, S. (2006) Cross-clade neutralizing activity of human anti-V3 monoclonal antibodies derived from the cells of individuals infected with non-B clades of human immunodeficiency virus type 1. *J. Virol.* **80**, 6865–6872
26. van Gils, M. J., and Sanders, R. W. (2013) Broadly neutralizing antibodies against HIV-1: templates for a vaccine. *Virology* **435**, 46–56
27. Eda, Y., Takizawa, M., Murakami, T., Maeda, H., Kimachi, K., Yonemura, H., Koyanagi, S., Shiosaki, K., Higuchi, H., Makizumi, K., Nakashima, T., Osatomi, K., Tokiyoshi, S., Matsushita, S., Yamamoto, N., and Honda, M. (2006) Sequential immunization with V3 peptides from primary human immunodeficiency virus type 1 produces cross-neutralizing antibodies against primary isolates with a matching narrow-neutralization sequence motif. *J. Virol.* **80**, 5552–5562
28. Matsushita, S., Takahama, S., Shibata, J., Kimura, T., Shiozaki, K., Eda, Y., Koito, A., Murakami, T., and Yoshimura, K. (2005) Ex vivo neutralization of HIV-1 quasi-species by a broadly reactive humanized monoclonal antibody KD-247. *Hum. Antibodies* **14**, 81–88
29. Eda, Y., Murakami, T., Ami, Y., Nakasone, T., Takizawa, M., Someya, K., Kaizu, M., Izumi, Y., Yoshino, N., Matsushita, S., Higuchi, H., Matsui, H., Shinohara, K., Takeuchi, H., Koyanagi, Y., Yamamoto, N., and Honda, M. (2006) Anti-V3 humanized antibody KD-247 effectively suppresses ex vivo generation of human immunodeficiency virus type 1 and affords sterile protection of monkeys against a heterologous simian/human immunodeficiency virus infection. *J. Virol.* **80**, 5563–5570
30. Murakami, T., Eda, Y., Nakasone, T., Ami, Y., Someya, K., Yoshino, N., Kaizu, M., Izumi, Y., Matsui, H., Shinohara, K., Yamamoto, N., and Honda, M. (2009) Postinfection passive transfer of KD-247 protects against simian/human immunodeficiency virus–induced $CD4^+$ T-cell loss in macaque lymphoid tissue. *AIDS* **23**, 1485–1494
31. Pflugrath, J. W. (1999) The finer things in X-ray diffraction data collection. *Acta Crystallogr. D Biol. Crystallogr.* **55**, 1718–1725
32. Matthews, B. W. (1985) Determination of protein molecular weight, hydration, and packing from crystal density. *Methods Enzymol.* **114**, 176–187
33. Vagin, A., and Teplyakov, A. (1997) MOLREP: an automated program for molecular replacement. *J. Appl. Cryst.* **30**, 1022–1025
34. Adams, P. D., Afonine, P. V., Bunkóczi, G., Chen, V. B., Davis, I. W., Echols, N., Headd, J. J., Hung, L. W., Kapral, G. J., Grosse-Kunstleve, R. W., McCoy, A. J., Moriarty, N. W., Oeffner, R., Read, R. J., Richardson, D. C., Richardson, J. S., Terwilliger, T. C., and Zwart, P. H. (2010) PHENIX: a comprehensive Python-based system for macromolecular structure solution. *Acta Crystallogr. D Biol. Crystallogr.* **66**, 213–221
35. Langer, G., Cohen, S. X., Lamzin, V. S., and Perrakis, A. (2008) Automated macromolecular model building for X-ray crystallography using ARP/wARP version 7. *Nat. Protoc.* **3**, 1171–1179
36. Murshudov, G. N., Vagin, A. A., and Dodson, E. J. (1997) Refinement of macromolecular structures by the maximum-likelihood method. *Acta Crystallogr. D Biol. Crystallogr.* **53**, 240–255
37. Emsley, P., Lohkamp, B., Scott, W. G., and Cowtan, K. (2010) Features and development of Coot. *Acta Crystallogr. D Biol. Crystallogr.* **66**, 486–501
38. Ong, Y. T., Kirby, K. A., Hachiya, A., Chiang, L. A., Marchand, B., Yoshimura, K., Murakami, T., Singh, K., Matsushita, S., and Sarafianos, S. G. (2012) Preparation of biologically active single-chain variable antibody fragments that target the HIV-1 gp120 V3 loop. *Cell. Mol. Biol. (Noisy-le-grand)* **58**, 71–79
39. Sreerama, N., and Woody, R. W. (1993) A self-consistent method for the analysis of protein secondary structure from circular dichroism. *Anal. Biochem.* **209**, 32–44

40. Sreerama, N., Venyaminov, S. Y., and Woody, R. W. (1999) Estimation of the number of alpha-helical and beta-strand segments in proteins using circular dichroism spectroscopy. *Protein Sci.* **8**, 370–380
41. Andrade, M. A., Chacón, P., Merelo, J. J., and Morán, F. (1993) Evaluation of secondary structure of proteins from UV circular dichroism spectra using an unsupervised learning neural network. *Protein Eng.* **6**, 383–390
42. Whitmore, L., and Wallace, B. A. (2004) DICHROWEB, an online server for protein secondary structure analyses from circular dichroism spectroscopic data. *Nucleic Acids Res.* **32**, W668-73
43. Whitmore, L., and Wallace, B. A. (2008) Protein secondary structure analyses from circular dichroism spectroscopy: methods and reference databases. *Biopolymers* **89**, 392–400
44. Janes, R. W. (2009) Reference datasets for protein ciruclar dichroism and synchrotron radiation circular dichroism spectroscopic analyses. In *Modern Techniques in Circular Dichroism and Synchrotron Radiation Circular Dichroism Spectroscopy*, Vol. 1, *Advances in Biomedical Spectroscopy* (Wallace, B. A., and Janes, R. W., eds.), pp. 183–201, IOS Press, Amsterdam, Netherlands
45. Shaw, G. M., Hahn, B. H., Arya, S. K., Groopman, J. E., Gallo, R. C., and Wong-Staal, F. (1984) Molecular characterization of human T-cell leukemia (lymphotropic) virus type III in the acquired immune deficiency syndrome. *Science* **226**, 1165–1171
46. Gallo, R. C., Salahuddin, S. Z., Popovic, M., Shearer, G. M., Kaplan, M., Haynes, B. F., Palker, T. J., Redfield, R., Oleske, J., Safai, B., et al. (1984) Frequent detection and isolation of cytopathic retroviruses (HTLV-III) from patients with AIDS and at risk for AIDS. *Science* **224**, 500–503
47. Montefiori, D. C. (2009) Measuring HIV neutralization in a luciferase reporter gene assay. *Methods Mol. Biol.* **485**, 395–405
48. Chen, V. B., Arendall III, W. B., Headd, J. J., Keedy, D. A., Immormino, R. M., Kapral, G. J., Murray, L. W., Richardson, J. S., and Richardson, D. C. (2010) MolProbity: all-atom structure validation for macromolecular crystallography. *Acta Crystallogr. D Biol. Crystallogr.* **66**, 12–21
49. Ramachandran, G. N., and Sasisekharan, V. (1968) Conformation of polypeptides and proteins. *Adv. Protein Chem.* **23**, 283–437
50. Stanfield, R. L., Zemla, A., Wilson, I. A., and Rupp, B. (2006) Antibody elbow angles are influenced by their light chain class. *J. Mol. Biol.* **357**, 1566–1574
51. Kabat, E. A., Wu, T. T., Perry, H. M., Gottesman, K. S., and Foeller, C. (1991) *Sequences of Proteins of Immunological Interest*, National Institutes of Health, Bethesda, MD
52. Abhinandan, K. R., and Martin, A. C. (2008) Analysis and improvements to Kabat and structurally correct numbering of antibody variable domains. *Mol. Immunol.* **45**, 3832–3839
53. Al-Lazikani, B., Lesk, A. M., and Chothia, C. (1997) Standard conformations for the canonical structures of immunoglobulins. *J. Mol. Biol.* **273**, 927–948
54. Shirai, H., Kidera, A., and Nakamura, H. (1996) Structural classification of CDR-H3 in antibodies. *FEBS Lett.* **399**, 1–8
55. Stanfield, R. L., Ghiara, J. B., Ollmann Saphire, E., Profy, A. T., and Wilson, I. A. (2003) Recurring conformation of the human immunodeficiency virus type 1 gp120 V3 loop. *Virology* **315**, 159–173
56. Ratner, L., Fisher, A., Jagodzinski, L. L., Mitsuya, H., Liou, R. S., Gallo, R. C., and Wong-Staal, F. (1987) Complete nucleotide sequences of functional clones of the AIDS virus. *AIDS Res. Hum. Retroviruses* **3**, 57–69
57. Javaherian, K., Langlois, A. J., LaRosa, G. J., Profy, A. T., Bolognesi, D. P., Herlihy, W. C., Putney, S. D., and Matthews, T. J. (1990) Broadly neutralizing antibodies elicited by the hypervariable neutralizing determinant of HIV-1. *Science* **250**, 1590–1593
58. Bell, C. H., Pantophlet, R., Schiefner, A., Cavacini, L. A., Stanfield, R. L., Burton, D. R., and Wilson, I. A. (2008) Structure of antibody F425-B4e8 in complex with a V3 peptide reveals a new binding mode for HIV-1 neutralization. *J. Mol. Biol.* **375**, 969–978
59. Burke, V., Williams, C., Sukumaran, M., Kim, S. S., Li, H., Wang, X. H., Gorny, M. K., Zolla-Pazner, S., and Kong, X. P. (2009) Structural basis of the cross-reactivity of genetically related human anti-HIV-1 mAbs: implications for design of V3-based immunogens. *Structure* **17**, 1538–1546
60. Jiang, X., Burke, V., Totrov, M., Williams, C., Cardozo, T., Gorny, M. K., Zolla-Pazner, S., and Kong, X. P. (2010) Conserved structural elements in the V3 crown of HIV-1 gp120. *Nat. Struct. Mol. Biol.* **17**, 955–961
61. Stanfield, R. L., Gorny, M. K., Williams, C., Zolla-Pazner, S., and Wilson, I. A. (2004) Structural rationale for the broad neutralization of HIV-1 by human monoclonal antibody 447-52D. *Structure* **12**, 193–204
62. Yoshimura, K., Shibata, J., Kimura, T., Honda, A., Maeda, Y., Koito, A., Murakami, T., Mitsuya, H., and Matsushita, S. (2006) Resistance profile of a neutralizing anti-HIV monoclonal antibody, KD-247, that shows favourable synergism with anti-CCR5 inhibitors. *AIDS* **20**, 2065–2073
63. Hatada, M., Yoshimura, K., Harada, S., Kawanami, Y., Shibata, J., and Matsushita, S. (2010) Human immunodeficiency virus type 1 evasion of a neutralizing anti-V3 antibody involves acquisition of a potential glycosylation site in V2. *J. Gen. Virol.* **91**, 1335–1345
64. Kessler, N., Zvi, A., Ji, M., Sharon, M., Rosen, O., Levy, R., Gorny, M., Zolla-Pazner, S., and Anglister, J. (2003) Expression, purification, and isotope labeling of the Fv of the human HIV-1 neutralizing antibody 447-52D for NMR studies. *Protein Expr. Purif.* **29**, 291–303
65. Brändén, C., and Tooze, J. (1999) *Introduction to Protein Structure*, Garland Science, New York
66. Greenfield, N., and Fasman, G. D. (1969) Computed circular dichroism spectra for the evaluation of protein conformation. *Biochemistry* **8**, 4108–4116
67. Eglen, R. M., Reisine, T., Roby, P., Rouleau, N., Illy, C., Bossé, R., and Bielefeld, M. (2008) The use of AlphaScreen technology in HTS: current status. *Curr. Chem. Genomics* **1**, 2–10
68. Sundberg, E. J. (2009) Structural basis of antibody-antigen interactions. *Methods Mol. Biol.* **524**, 23–36
69. Stanfield, R. L., Gorny, M. K., Zolla-Pazner, S., and Wilson, I. A. (2006) Crystal structures of human immunodeficiency virus type 1 (HIV-1) neutralizing antibody 2219 in complex with three different V3 peptides reveal a new binding mode for HIV-1 cross-reactivity. *J. Virol.* **80**, 6093–6105
70. Gorny, M. K., Xu, J. Y., Karwowska, S., Buchbinder, A., and Zolla-Pazner, S. (1993) Repertoire of neutralizing human monoclonal antibodies specific for the V3 domain of HIV-1 gp120. *J. Immunol.* **150**, 635–643
71. Julien, J. P., Cupo, A., Sok, D., Stanfield, R. L., Lyumkis, D., Deller, M. C., Klasse, P. J., Burton, D. R., Sanders, R. W., Moore, J. P., Ward, A. B., and Wilson, I. A. (2013) Crystal structure of a soluble cleaved HIV-1 envelope trimer. *Science* **342**, 1477–1483
72. Gorny, M. K., Revesz, K., Williams, C., Volsky, B., Louder, M. K., Anyangwe, C. A., Krachmarov, C., Kayman, S. C., Pinter, A., Nadas, A., Nyambi, P. N., Mascola, J. R., and Zolla-Pazner, S. (2004) The v3 loop is accessible on the surface of most human immunodeficiency virus type 1 primary isolates and serves as a neutralization epitope. *J. Virol.* **78**, 2394–2404

Received for publication June 6, 2014.
Accepted for publication August 26, 2014.

Journal of General Virology (2014), **95**, 1816–1826 DOI 10.1099/vir.0.062885-0

Impact of maraviroc-resistant and low-CCR5-adapted mutations induced by *in vitro* passage on sensitivity to anti-envelope neutralizing antibodies

Kazuhisa Yoshimura,[1,2]† Shigeyoshi Harada,[1,2]† Samatchaya Boonchawalit,[1,2] Yoko Kawanami[2] and Shuzo Matsushita[2]

Correspondence
Kazuhisa Yoshimura
ykazu@nih.go.jp
Shuzo Matsushita
shuzo@kumamoto-u.ac.jp

[1]AIDS Research Centre, National Institute of Infectious Diseases, 1-23-1 Toyama, Shinjuku-ku, Tokyo 162-8640, Japan

[2]Center for AIDS Research, Kumamoto University, 2-2-1 Honjo, Chuo-ku, Kumamoto 860-0811, Japan

The aim of this study was to generate maraviroc (MVC)-resistant viruses *in vitro* using a human immunodeficiency virus type 1 subtype B clinical isolate (HIV-1_{KP-5}) to understand the mechanism(s) of resistance to MVC. To select HIV-1 variants resistant to MVC *in vitro*, we exposed high-chemokine (C-C motif) receptor 5 (CCR5)-expressing PM1/CCR5 cells to HIV-1_{KP-5} followed by serial passage in the presence of MVC. We also passaged HIV-1_{KP-5} in PM1 cells, which were low CCR5 expressing to determine low-CCR5-adapted substitutions and compared the Env sequences of the MVC-selected variants. Following 48 passages with MVC (10 μM), HIV-1_{KP-5} acquired a resistant phenotype [maximal per cent inhibition (MPI) 24 %], whilst the low-CCR5-adapted variant had low sensitivity to MVC (IC_{50} ~200 nM), but not reduction of the MPI. The common substitutions observed in both the MVC-selected and low-CCR5-adapted variants were selected from the quasi-species, in V1, V3 and V5. After 14 passages, the MVC-selected variants harboured substitutions around the CCR5 N-terminal-binding site and V3 (V200I, T297I, K305R and M434I). The low-CCR5-adapted infectious clone became sensitive to anti-CD4bs and CD4i mAbs, but not to anti-V3 mAb and autologous plasma IgGs. Conversely, the MVC-selected clone became highly sensitive to the anti-envelope (Env) mAbs tested and the autologous plasma IgGs. These findings suggest that the four MVC-resistant mutations required for entry using MVC-bound CCR5 result in a conformational change of Env that is associated with a phenotype sensitive to anti-Env neutralizing antibodies.

Received 15 December 2013
Accepted 29 April 2014

INTRODUCTION

Human immunodeficiency virus type 1 (HIV-1) entry into target cells is triggered by the interaction of the viral envelope glycoproteins (Env) with its receptor CD4 and one or two major coreceptors, chemokine (C-C motif) receptor 5 (CCR5) or chemokine (C-X-C motif) receptor 4 (CXCR4), and culminates in fusion of the viral and cell membranes. Env is organized into trimers on virions, and consists of the gp120 surface and gp41 transmembrane subunits (Wyatt & Sodroski, 1998). The small-molecule CCR5 antagonist maraviroc (MVC) was the first CCR5 inhibitor licensed for clinical use (Gulick *et al.*, 2008). CCR5 inhibitors work by allosterically altering the conformation of CCR5 at the cell surface, thereby disrupting its interaction with HIV gp120 (Berger *et al.*, 1999; Dorr *et al.*, 2005). Although MVC and another CCR5 inhibitor, vicriviroc (VCV), can efficiently suppress HIV-1 replication, resistant variants can arise both *in vitro* and *in vivo*, and these resistant viruses are adapted to use drug-bound CCR5 for entry (Berro *et al.*, 2009; Kuhmann *et al.*, 2004; Marozsan *et al.*, 2005; Ogert *et al.*, 2009, 2010; Ratcliff *et al.*, 2013; Roche *et al.*, 2011b; Tilton *et al.*, 2010; Tsibris *et al.*, 2008; Westby *et al.*, 2007; Yuan *et al.*, 2011; Yusa *et al.*, 2005). Current models of gp120 binding to a coreceptor suggest that the crown of the gp120 V3 loop interacts principally with the second extracellular loop region of the coreceptor, whilst the gp120 bridging sheet, which is formed after CD4 binding, and the stem of the V3 loop interact with the N terminus of the coreceptor (Brelot *et al.*, 1999; Cormier & Dragic, 2002; Farzan *et al.*, 1999; Huang *et al.*, 2005). The development of resistance is an important issue for HIV treatment regimens incorporating MVC, as is the case for any antimicrobial agent.

†These authors contributed equally to this work.

The GenBank/EMBL/DDBJ accession numbers for the envelope sequences of KP-5 are AB742145–AB742157.

Three supplementary figures are available with the online version of this paper.

HIV-1 can develop clinical resistance to CCR5 antagonists by two routes. The first pathway is through emergence of pre-existing CXCR4-using viruses (Fätkenheuer *et al.*, 2008; Landovitz *et al.*, 2008; Westby *et al.*, 2006). CCR5 inhibitor evasion can also occur by the accumulation of multiple mutations in gp120 and/or gp41 without a switch in coreceptor usage (Dragic *et al.*, 2000; Maeda *et al.*, 2006, 2008a; Roche *et al.*, 2011b; Tsamis *et al.*, 2003). The resistant pathway is characterized not by shifts in IC_{50} (a competitive inhibitor), but rather by reductions in the maximal per cent inhibition (MPI). Reductions in MPI are due to the resistant virus developing the ability to bind to the antagonist-modified form of CCR5 (Westby *et al.*, 2007). However, one study reported that chimeric clones bearing the N425K mutation in C4 replicated at high MVC concentrations and displayed significant shifts in IC_{50}s, characteristic of resistance to all other antiretroviral drugs, but not MVC (Ratcliff *et al.*, 2013).

Escape mutants to the CCR5 inhibitor, AD101 (SCH-350581), have been found to be more sensitive than the parental isolate to a subset of neutralizing mAbs against V3 and a CD4-induced (CD4i) epitope (Pugach *et al.*, 2007; Berro *et al.*, 2009). To date, however, it is not clear which mutation(s) induced by MVC affect the accessibility of neutralizing mAbs to the epitopes in Env.

Therefore, to determine the resistance mechanisms to MVC, we passaged a primary CCR5-tropic (R5) subtype B isolate in the high-CCR5-expressing T-cell line PM1/CCR5 in the presence of MVC (Fig. S1, available in the online Supplementary Material) and compared the Env sequences of variants with those cultured in the low-CCR5-expressing parental PM1 cell line (Fig. S1). We also investigated the phenotypic change in the MVC-resistant clone against anti-Env antibodies, especially for anti-V3 neutralizing mAbs and autologous plasma IgGs, and compared the results with the low-CCR5-adapted clone to determine the key mutations for accessibility of neutralizing mAbs to the epitopes in Env.

RESULTS

Anti-HIV-1 activities of MVC toward laboratory strains and primary HIV-1 isolates

Initially, we determined the MPI and the IC_{50} values of MVC against different laboratory-adapted and primary HIV-1 isolates, including both CXCR4-tropic (X4) and R5 viruses. MVC inhibited the laboratory-adapted HIV-1 R5 strains HIV-1_{BaL} and HIV-$1_{JR\text{-}FL}$ with MPIs of 98 and 97 %, respectively, but did not inhibit the X4 virus HIV-1_{IIIB} or dual-tropic virus HIV-$1_{89.6}$ (MPI <20 %, Table 1). We also tested MVC against 14 R5 primary isolates, including subtypes B, C and G, and the circulating recombinant form CRF08_BC. MVC effectively inhibited all of these primary isolates at concentrations of 1.2–26 nM (MPI 92–100 %), but did not inhibit three primary X4 isolates (two CRF01_AE and one subtype B) with MPI <20 % (Table 1).

Table 1. Inhibitory activities of MVC toward infection by laboratory-adapted and primary strains of HIV-1

Virus	Subtype	IC_{50}* (nM)	MPI (%)
Laboratory adapted			
R5			
HIV-1_{BaL}	B	26	98
HIV-$1_{JR\text{-}FL}$	B	6.9	97
Dual			
HIV-$1_{89.6}$	B	>1000	<20
X4			
HIV-1_{IIIB}	B	>1000	<20
Primary			
R5			
HIV-$1_{KP\text{-}5}$	B	26	92
HIV-$1_{KP\text{-}2}$	CRF08_BC	24	95
HIV-$1_{KP\text{-}6}$	G	20	95
HIV-$1_{KP\text{-}7}$	B	18	95
HIV-$1_{KP\text{-}8}$	B	14	97
HIV-$1_{KP\text{-}9}$	B	13	96
HIV-$1_{KP\text{-}10}$	B	9.2	98
HIV-$1_{KP\text{-}11}$	C	8.6	96
HIV-$1_{KP\text{-}12}$	B	5.1	98
HIV-$1_{KP\text{-}13}$	B	4.0	96
HIV-$1_{KP\text{-}14}$	B	3.0	95
HIV-$1_{KP\text{-}15}$	B	3.0	94
HIV-$1_{KP\text{-}16}$	B	2.2	100
HIV-$1_{KP\text{-}17}$	B	1.2	98
X4/mix			
HIV-$1_{KP\text{-}18}$	CRF01_AE	>1000	<20
HIV-$1_{KP\text{-}19}$	CRF01_AE	>1000	<20
HIV-$1_{KP\text{-}20}$	B	>1000	<20

*PM1/CCR5 cells (2×10^3) were exposed to 100 $TCID_{50}$ of each virus and then cultured in the presence of various concentrations of MVC. The IC_{50} values were determined by the WST-8 assay using a Cell Counting kit-8 on day 7 of culture. All assays were conducted in duplicate or triplicate.

Selection of MVC-resistant variants

To select MVC-resistant HIV-1 variants *in vitro*, we exposed PM1/CCR5 cells to HIV-$1_{KP\text{-}5}$, which had the highest IC_{50} value (26 nM) and lowest MPI (92 %) among the primary isolates tested, and serially passaged the viruses in the presence of increasing concentrations of MVC. As a control, HIV-$1_{KP\text{-}5}$ was passaged under the same conditions without MVC in PM1/CCR5 cells (designated the passage control). Moreover, to compare the differences between the MVC-resistant variant and low-CCR5-expressing-cell-adapted variant, we passaged HIV-$1_{KP\text{-}5}$ in low-CCR5-expressing parental PM1 cells (designated low-CCR5-adapted). The selected virus was initially propagated in the presence of 1 nM MVC and during the course of the selection procedure the concentration of MVC was increased to 10 μM over 48 passages (Fig. 1a).

Resistance to small-molecule CCR5 inhibitors is known to vary according to the cell type used (Anastassopoulou

et al., 2009; Ogert *et al.*, 2008; Pugach *et al.*, 2007; Westby *et al.*, 2007). To characterize the resistance profiles of the passaged variants, we tested the sensitivities of the three variants and HIV-1_{BaL} to MVC in phytohaemagglutinin (PHA)-activated PBMCs (Fig. 1b). The MPI of the MVC-resistant variant was lower than the MPIs of the passage control, low-CCR5-adapted variant and HIV-1_{BaL} (MPI 80.3 versus 92.3, 94.5 and 95.7 %, respectively).

The MVC-selected variant became highly resistant to MVC (Fig. 2), with an MPI of 24 % at 48 passages. However, the low-CCR5-adapted variant, which was passaged in PM1 cells, became low sensitive to MVC compared with the passage control (IC_{50} 279 versus 26.3 nM), but we did not find a reduction in the MPI.

We also determined the sequential MPIs and IC_{50} values of each passaged variant to MVC (Fig. 2). From passages

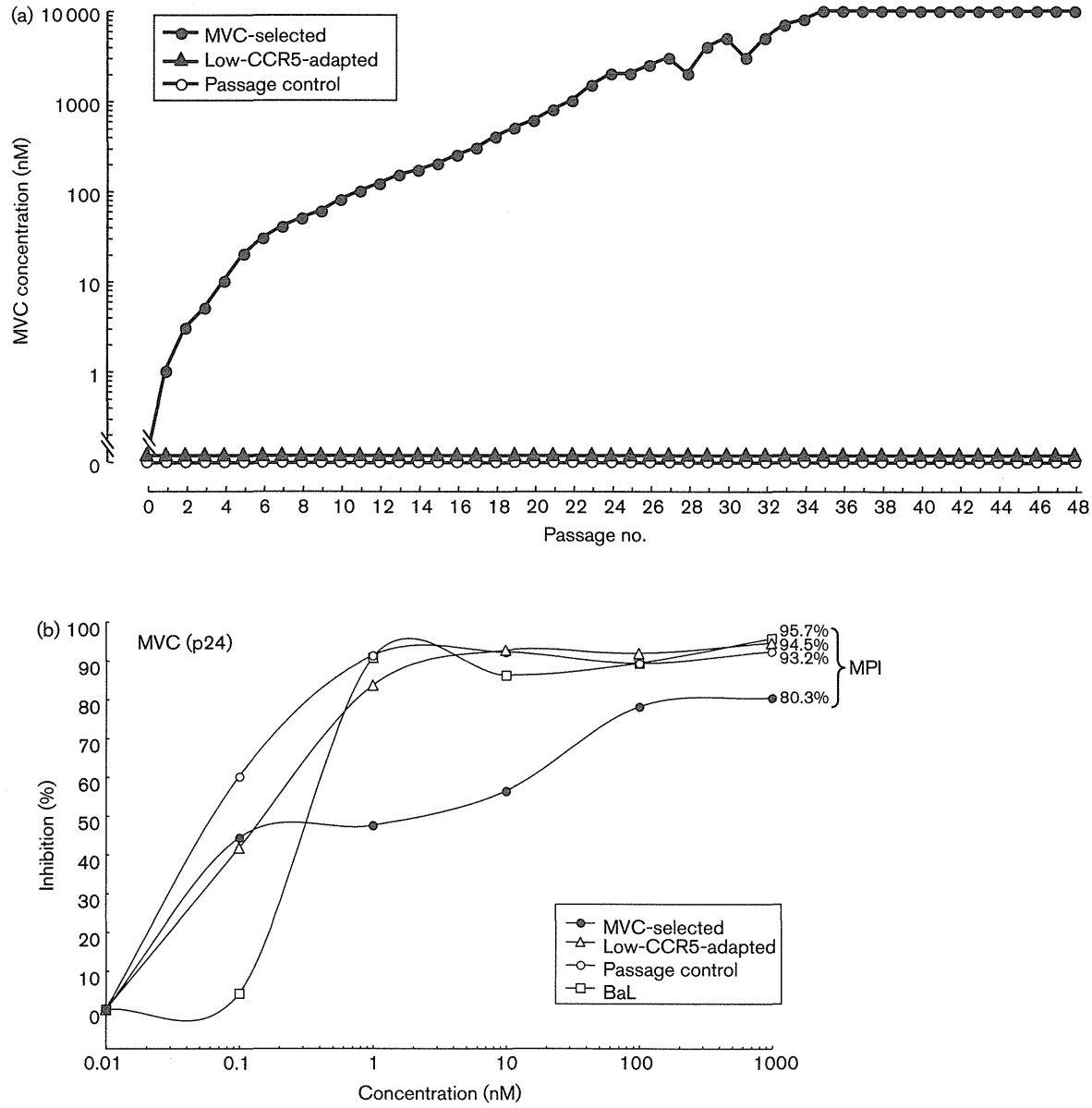

Fig. 1. Selection of MVC-resistant and low-CCR5-adapted virus variants. (a) The selection was carried out in PM1/CCR5 and PM1 cells as described in Methods. (b) Sensitivities of the MVC-selected (48 passages), low-CCR5-adapted (48 passages), passage control (48 passages) variants and HIV-1_{BaL} (BaL) to MVC as determined by p24 antigen measurement. PHA-activated PBMCs (1×10^6 cells ml^{-1}) were exposed to 100 $TCID_{50}$ of each variant and cultured in the presence or absence of various concentrations of the drug in 96-well microculture plates. The amounts of p24 antigen produced by the cells were determined on day 7. All assays were performed in triplicate.

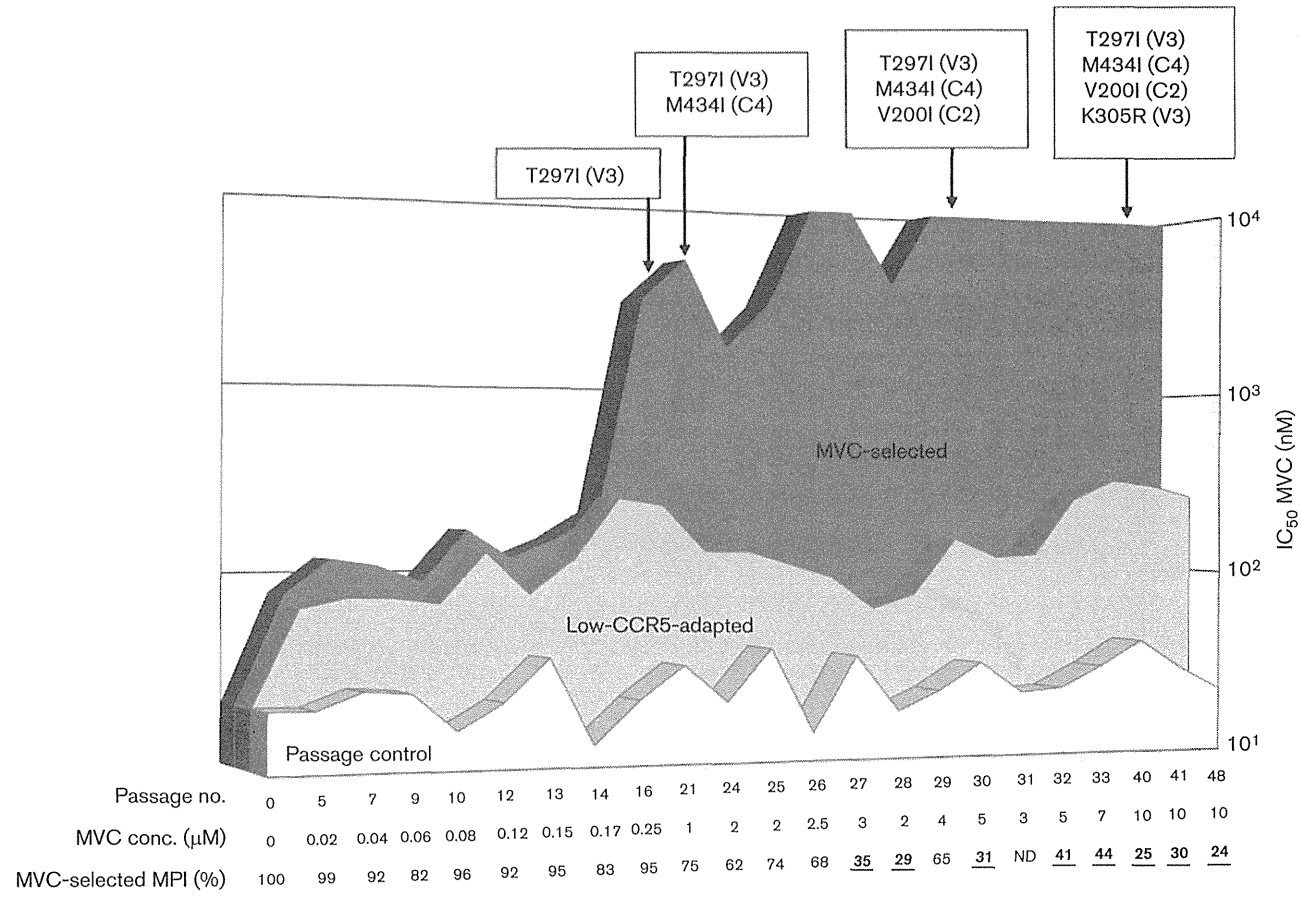

Fig. 2. Susceptibility of passaged variants to MVC. The sensitivity and MPI of each passaged variant to MVC was determined by a multi-round assay using the WST-8 assay as described in Methods. The *x*-axis shows the passage number, concentration of MVC (μM) and MPI values. The mutations observed in the highly MVC-resistant variants are shown above the graph.

1 to 14, the MVC-selected and low-CCR5-adapted variants had almost equal IC_{50} values and the MPIs were high. After 16 passages, the IC_{50} values of the MVC-selected variants continued to increase to >10 μM, whilst the MPIs decreased to 24% at 48 passages, especially after 27 passages. The low-CCR5-adapted variants maintained an IC_{50} value of ~200 nM and high MPIs (90–100%) until the end of the experiment (passage 48). Conversely, the passage control variants did not show remarkable changes in their IC_{50} values and MPIs throughout the passages (IC_{50} values of ~20 nM, MPI 95–100%). The low-CCR5-adapted variant was also resistant to two other CCR5 inhibitors, APL and TAK-779 (data not shown).

These findings suggested that the phenotype of the MVC-selected variants under low concentrations of the drug corresponded with that of the low-CCR5-adapted variants until 14 passages; then, under high concentrations, the MVC-selected variants acquired additional mutations for high resistance to the CCR5 inhibitor.

Comparison of the Env region sequences of the MVC-selected and low-CCR5-adapted mutants

To determine the genetic basis of the resistance in the HIV-1_{KP-5} variants and compare the substitutions between the MVC-selected and low-CCR5-adapted variants, the Env genes were sequenced (Figs 3, 4 and S2). At 17 passages, all substitutions in both the MVC-selected and low-CCR5-adapted variants were selected from the baseline viruses. Five of these substitutions in gp120, i.e. K8R, C11W (signal peptide), D141N (V1), E321D (V3) and I463T (V5), were observed in both passaged variants. Conversely, at positions 137 (K or E), 148 (Q or K) and 187 (G or D), the amino acids differed between the MVC-selected and low-CCR5-adapted variants. After 16 passages, the MVC-selected variants acquired four additional mutations, i.e. T297I (V3), M434I (C4), V200I (C2) and K305R (V3), at passages 17, 21, 34 and 41, respectively, which were not observed in the low-CCR5-adapted variants (Figs 2–4 and S2). After acquisition of M434I in C4 (21 passages), the MPI of the MVC-selected variants decreased gradually

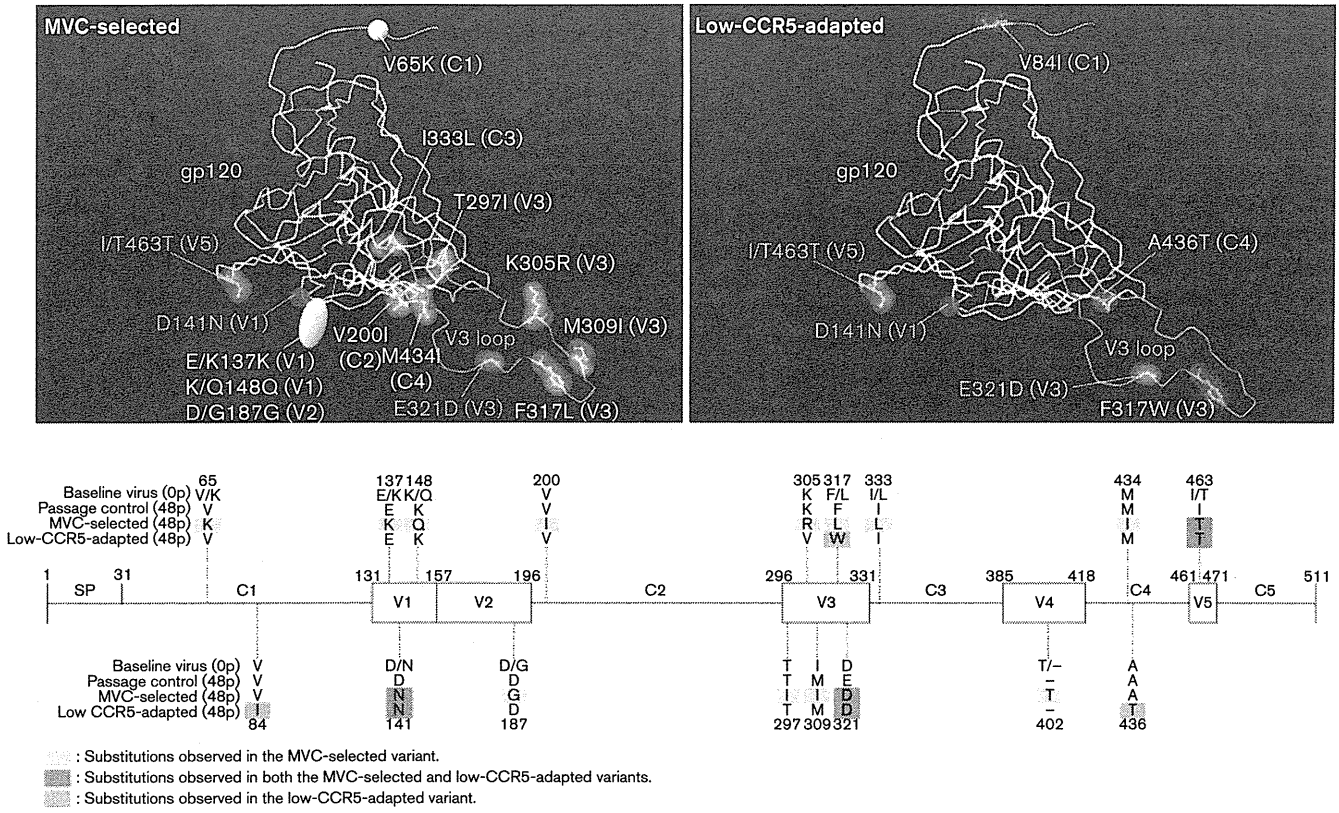

Fig. 3. Comparison of the locations of the mutations in the MVC-selected and low-CCR5-adapted gp120. The side chains of the mutated residues that appeared during the MVC selection (left) and low CCR5 adaptation (right) are shown in yellow (only MVC selection), pink (only low CCR5 adaptation) and green (both). A summary schema is also provided.

(from 74 to 24 %) (Fig. 2). The most important amino acid substitution for the reduction in the MPI might be K305R, because the MPI of the variant cultured without MVC after 48 passages increased by reverting from R to K at position 305 (data not shown). Three additional mutations, i.e. F317W (V3), V84I (C1) and A436T (C4), were observed in the low-CCR5-adapted variants at 17, 21 and 48 passages, respectively. These mutations might be compensatory for viral fitness following culture in the low-CCR5-expressing cells, because the MPIs of the variants with these three mutations did not differ from those of the variants prior to the acquisition of these mutations (>90 %).

These findings suggest that under low concentrations of MVC, the variants were selected from the baseline viruses similarly to the low-CCR5-adapted variants (IC_{50} shift and high MPI), whilst under high concentrations of the drug, the selected variants required additional mutations to use drug-bound coreceptors for entry into the target cells.

To compare the two mutation profiles obtained from the MVC-selected and low-CCR5-adapted variants at 48 passages, the crystal structure of gp120 was used (Figs 3 and 4). Comparison of the sequences of the two passaged variants based on the Protein Data Bank (PDB ID: 2B4C) crystal structure of gp120 showed that the MVC-selected variant harboured many substitutions within and around the V3 region, i.e. the CCR5 N-terminal-binding site, compared with the low-CCR5-adapted variant in the three-dimensional (3D) position. In a magnification of the CCR5 N-terminal-binding site (Fig. 4), three of four mutations, i.e. T297I, M434I and V200I, were concentrated around the V3 base and finally K305R appeared in the V3 stem region after 41 passages.

To determine the positions of MVC-selected mutations in the gp120 trimer form, we illustrated the sites of mutations on the structure of the BG505 SOSIP trimer obtained from the PDB (ID: 3J5M) (Fig. S3) (Lyumkis *et al.*, 2013). Almost all of the MVC-selected mutations occurred at the upper and outer side of the trimer. Several MVC-selected mutations, i.e. V65K, V200I, K305R, M309I, F317L and M434I, lay relatively close to the neighbouring gp120. These findings demonstrated that these mutations may affect trimer formation and expose neutralizing antibody epitopes.

Susceptibilities of the infectious clones with mutant Env to anti-Env mAbs

In a previous study, a CCR5 inhibitor (AD101)-resistant infectious clone was sensitive to neutralization via V3 and

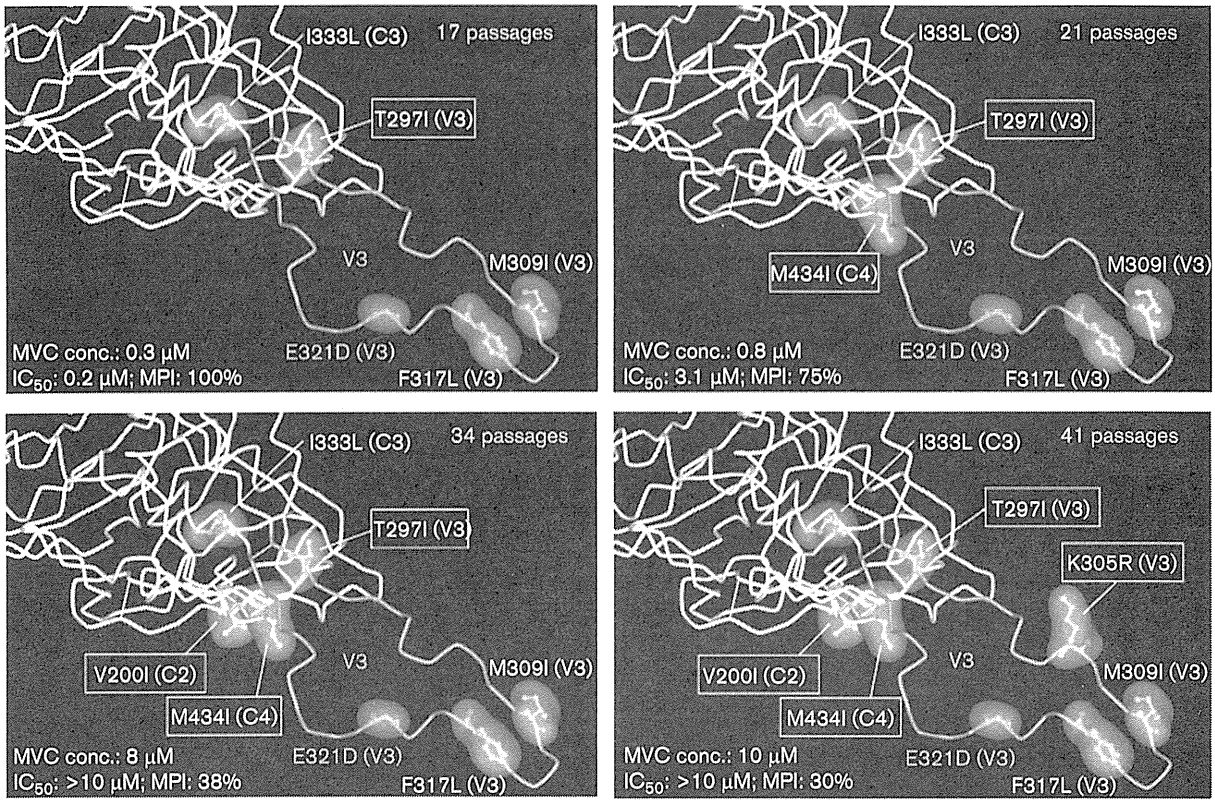

Fig. 4. Enlargement of the area of the CCR5 N-terminal-binding site and V3 loop in gp120. The side chains of the mutated residues that appeared during *in vitro* selection with MVC at 17 (upper left), 21 (upper right), 34 (lower left) and 41 passages (lower right) are shown. The crystal structure of gp120 was retrieved from the Protein Data Bank (PDB ID: 2B4C).

CD4i epitopes (Berro *et al.*, 2009). To examine whether our three passaged variants became sensitive to anti-Env mAbs, we constructed three infectious clones with each 48-passaged Env (Fig. 5). The clone with the Env of the MVC-selected variant showed a low MPI (56 %) under a high concentration of MVC, which was also seen with the passage control and low-CCR5-adapted clones (Fig. 5a). Using these infectious clones, we tested the susceptibilities to the anti-Env mAbs b12 [anti-CD4 binding site (anti-CD4bs)], 4E9C (anti-CD4i) and KD-247 (anti-V3). As shown in Fig. 5(b), the MVC-selected and low-CCR5-adapted clones showed higher sensitivity to b12 than the passage control clone, with IC_{50} values of 0.22, 0.31 and 0.86 μg ml^{-1}, respectively. The MVC-selected and low-CCR5-adapted clones became highly sensitive to 4E9C compared with the passage control clone (IC_{50} values of 0.08, 0.41 and >5 μg ml^{-1}, respectively) (Fig. 5c). Moreover, the clone with the MVC-selected Env was highly sensitive to anti-V3 mAb KD-247, while the low-CCR5-adapted and passage control clones were not (IC_{50} values of 0.04, >100 and >100 μg ml^{-1}, respectively) (Fig. 5d).

These findings indicated that the MVC-selected clone with its greater number of mutations might contribute to exposure of neutralizing epitopes for these three mAbs, whilst the low-CCR5-adapted mutations could change the conformation of Env to become sensitive to anti-CD4i and CD4bs mAbs, but not anti-V3 mAb.

Susceptibilities of the infectious clones with mutant Env to autologous plasma IgGs

We also examined whether the infectious clones with the passaged Env mutations were neutralized by autologous plasma IgGs. As shown in Fig. 6(a), none of the autologous plasma IgGs could neutralize the passage control clone at concentrations up to 100 μg ml^{-1}. In the low-CCR5-adapted clone, some of the plasma IgGs slightly inhibited the replication of the virus under high concentrations, but did not reach the 50 % inhibition level (Fig. 6b). Conversely, all seven plasma IgGs were able to completely neutralize the clone with the MVC-selected Env (IC_{50} 2.6–37 μg ml^{-1}, MPI 79–97 %) (Fig. 6c).

These findings show that the MVC-selected clone with the greater number of mutations also might contribute to exposure of neutralizing epitopes for autologous plasma IgGs.

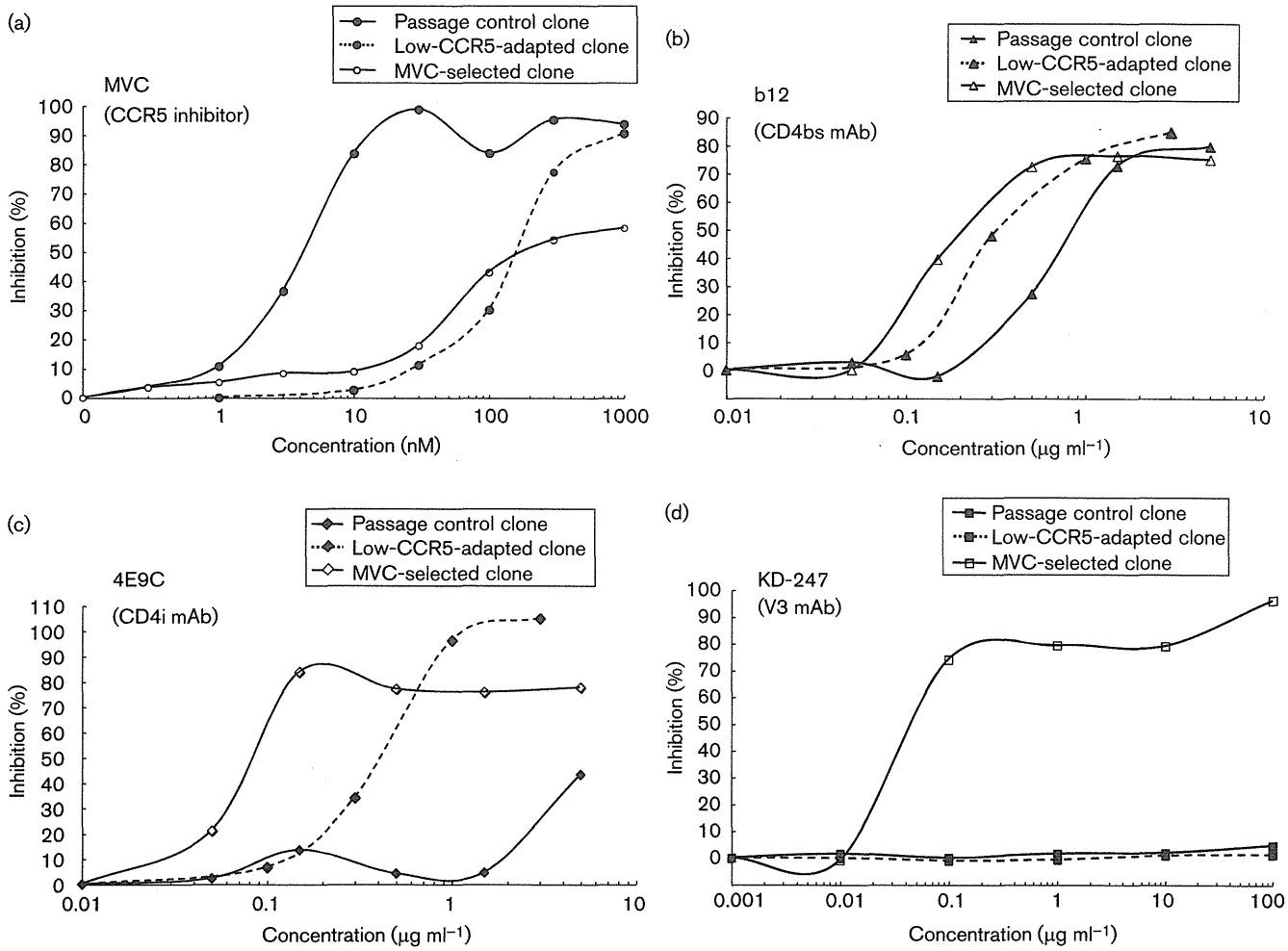

Fig. 5. Sensitivities of infectious clones with the passage control, low-CCR5-adapted and MVC-selected Env mutations to MVC and anti-Env mAbs. The sensitivities of the infectious clones with the passage control (filled symbols), low-CCR5-adapted (filled symbols and dotted lines) and MVC-selected (open symbols) Env mutations to (a) MVC, (b) b12, (c) 4E9C and (d) KD-247 are shown. The sensitivities of each infectious clone to MVC and mAbs were determined by the WST-8 assay as described in Methods. All assays were conducted in duplicate.

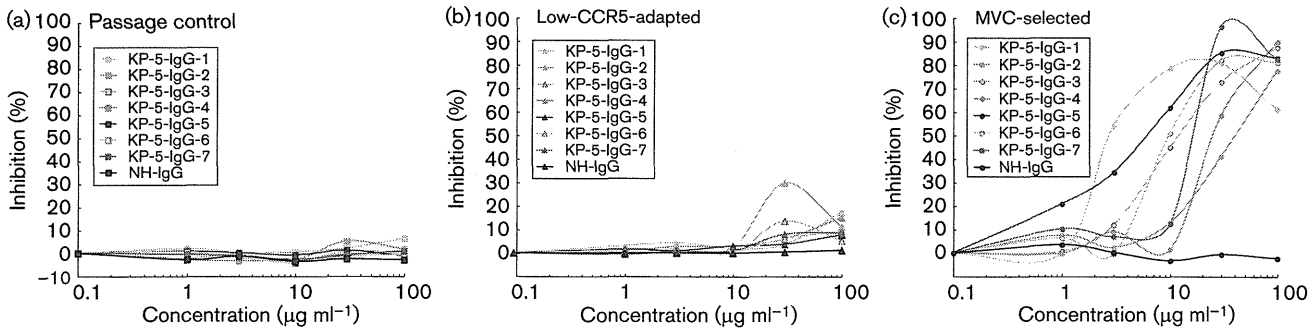

Fig. 6. Sensitivities of infectious clones with the passage control, low-CCR5-adapted and MVC-selected Env mutations to autologous plasma IgGs. The sensitivities of the infectious clones with the (a) passage control, (b) low-CCR5-adapted and (c) MVC-selected Env mutations to seven autologous plasma IgGs (KP-5-IgG-1 to KP-5-IgG-7; coloured symbols) and normal human plasma IgG (NH-IgG; black symbols) are shown. The sensitivity of each infectious clone to the plasma IgGs was determined by the WST-8 assay as described in Methods. All assays were conducted in duplicate.

DISCUSSION

The CCR5 inhibitors, MCV and VCV, are allosteric inhibitors of virus entry, hence resistance to these drugs is evidenced by a reduction in the plateau of virus inhibition curves rather than by increases in IC_{50} (Dragic *et al.*, 2000; Maeda *et al.*, 2006, 2008a; Roche *et al.*, 2011b; Tsamis *et al.*, 2003). One study reported that resistant mechanisms contribute to the altered recognition of drug-bound CCR5 by an MVC-resistant HIV-1 strain. This study demonstrated very efficient usage of drug-bound CCR5, characterized by increased dependence on the CCR5 N terminus (Tilton *et al.*, 2010). Another report demonstrated a similar yet distinct mechanism of escape from MVC by MVC-resistant Env, with comparatively less efficient usage of drug-bound CCR5 (Roche *et al.*, 2011b). In the absence of the drug, MVC-resistant Env maintains a highly efficient interaction with CCR5, similar to that of MVC-sensitive Env, and displays a relatively modest increase in dependence on the CCR5 N terminus (Roche *et al.*, 2011b). However, in the presence of the drug, MVC-resistant Env interacts much less efficiently with CCR5 and becomes critically dependent on the CCR5 N terminus. In the current study, we induced MVC-resistant HIV-1, which harboured many substitutions within and around the V3 region, i.e. the CCR5 N-terminal-binding site *in vitro*. In order to determine whether the resistant variant displayed an increased CCR5 N-terminal dependence, we determined the sensitivity of each variant to anti-CCR5 N-terminal mAb, CTC-5. All passaged variants were completely resistant to CTC-5; however, the MVC-selected variant became sensitive to CTC-5 when MVC (1 μM) was added in the assay, as reported previously (Berro *et al.*, 2009). These results suggest that the four mutations associated with the CCR5-binding site in the MVC-selected variant might create an increased dependency on interaction with the CCR5 N terminus.

In this study, we attempted to determine the difference between the MVC-selected and low-CCR5-adapted variants in parallel using an *in vitro* passage system. Under low concentrations of MVC, the MPI reduction was not observed in either the MVC-selected variant or the low-CCR5-adapted variant, although both passaged variants had common substitutions in the V1, V3 and V5 regions from quasi-species. Compared with the baseline viruses, under high concentrations of MVC, the resistant variants acquired mutations within the area of the CCR5-binding site in gp120 by evolution and/or selection from minor subsets. Following acquisition of the latter mutations, the variants with mutant Env showed a considerably reduced MPI (24 %). These results indicate that mutants arising from passage in low-CCR5-expressing cells can influence the IC_{50} shift, but not a reduction in the MPI.

One previous study showed that although numerous changes were observed in V3 and other regions of gp160, genotypic analysis of the cloned *env* sequences revealed no specific mutational pattern associated with reduced susceptibility to VCV in a phase 2 clinical trial (Pantophlet & Burton, 2006). Using the Los Alamos Database, we found that the frequencies of the four mutations occurred in <10 % of 1501 subtype B viruses (V200I, 5.1 %; T297I, 5.9 %; K305R, 9.5 %; M434I, 2.5 %). Assays for these mutations might provide useful clinical markers for determining the sensitivity of HIV-1 to MVC. One limitation of the present study was that only one primary isolate was used and a single *in vitro* passage series was used for variant selection. Further studies using multiple isolates and multiple passage cultures are required to determine if this MVC-susceptibility model applies to other HIV subtypes and cell systems. Ogert *et al.* (2009) and Anastassopoulou *et al.* (2009) reported that multistep resistance mutations during *in vitro* selection that reduced the MPI values to VCV were driven by the K305R substitution and the H308P substitution was related to a reduction in the MPI plateau level to VCV resistance. Henrich *et al.* (2010) also reported such mutations *in vivo*, as S306P was not detected in the baseline virus population, but was necessary for maximal resistance when incorporated into V3 backbones that included pre-existing VCV resistance mutations. Our *in vitro* study also showed that the K305R mutation contributed to maximal resistance to MVC when incorporated into V3 and CCR5 N-terminal-binding site backbones that included pre-existing MVC resistance mutations. Moreover, our MVC-selected variant with MVC (1 μM) became sensitive to the CCR5 N-terminal mAb (data not shown). Conversely, Roche *et al.* (2011a) reported that the MVC-resistant variants increased reliance on sulfated tyrosine residues in the CCR5 N terminus without common gp120 resistance mutations. One resistant clone (17-Res) harboured I317F, A322D and I323V substitutions in the V3 loop, whilst the other resistant clone (24-Res) had P308S and Ala inserted at the 313 position in the V3. In our MVC-resistant variant, we found some mutations at the same positions (305, 309, 317 and 321) in the V3 region as those of 17-Res and 24-Res clones (Roche *et al.*, 2011a). It is still not clear whether such mutations around the V3 loop stem region contribute to increased reliance on the CCR5 N terminus, and further studies are needed to determine the relationship between each mutation and CCR5 N terminus dependency.

HIV Env evades antibody recognition of conserved epitopes by several means, including decoration with a dense glycan shield, hypervariable loops that mask conserved features and high intrinsic conformational dynamics that render it a poorly defined antigen (Pantophlet & Burton, 2006). In the present study, the infectious clone with the Env of the low-CCR5-adapted virus became sensitive to anti-CD4i mAb, but not anti-V3 mAb and autologous plasma IgGs. Conversely, the clone with the highly MVC-resistant Env was neutralized by the anti-V3 mAb at low concentrations (<0.1 μg ml^{-1}) and also by the autologous plasma IgGs. These findings suggest that the low-CCR5-adapted mutations are related to accessibility of the anti-CD4i mAb to its epitopes, whilst the greater number of mutations in the MVC-selected virus may provide access to the epitopes of

not only anti-CD4bs and anti-CD4i mAbs, but also the anti-V3 mAb and autologous plasma IgGs. In preliminary data, we have confirmed the presence of such anti-CD4i and anti-V3 antibodies in plasma samples from the subject from whom HIV-1_{KP-5} was isolated (unpublished data). *In vivo*, where potent levels of Env neutralizing antibodies may be present, the MVC-selected variants may become neutralization-sensitive and not survive. For this reason, it is possible that CCR5 inhibitors, such as MVC, suppress HIV replication for long periods, especially in patients with high levels of circulating anti-Env neutralizing antibodies prior to treatment with MVC.

As some of the mutations in the MVC-selected variant are close to the epitope for KD-247, those mutations might influence the sensitivity and/or binding affinity to KD-247. Moreover, the mutations around and within the V3 loop may also affect the association with the V2 loop by opening of the trimer. Our study did not allow us to distinguish this possibility. Thus, further studies with single and combinations of mutations in Env to determine the binding affinity to the neutralizing antibodies by FACS and/or ELISA are ongoing.

Following CD4 binding, the CD4-binding site on gp120 becomes ordered and the bridging sheet subdomain forms, drawing the V1/V2 loops into a 'down' orientation and positioning them alongside CD4 (Guttman *et al.*, 2012). The MVC-selected variant in our study became highly sensitive to anti-CD4i and V3 neutralizing mAbs compared with the passage control virus. Further analysis of the effect of the CCR5 inhibitor-resistant Env to neutralizing antibodies would be of interest because, as reported in our previous work (Yoshimura *et al.*, 2006), the anti-V3 mAb KD-247-resistant variant became highly sensitive to CCR5 inhibitors.

METHODS

Viruses. Primary HIV-1 viruses were isolated from patients and passaged in PHA-activated PBMCs. Infected PBMCs were co-cultured for 5 days with PM1/CCR5 cells and the culture supernatants were stored at −150 °C until use (Yoshimura *et al.*, 2010). HIV-1_{KP-5} was isolated from a subject prior to MVC therapy but who has subsequently been taking combination antiretroviral therapy containing MVC since September 2009. The HIV-1_{KP-5} was isolated before starting the combination antiretroviral therapy.

Cells, culture conditions and reagents. The $CD4^+$ T-cell line PM1 (Lusso *et al.*, 1995) was obtained through the AIDS Research and Reference Reagent Program (ARRRP). The PM1/CCR5 cell line was a kind gift from Dr Yosuke Maeda (Kumamoto University, Kumamoto, Japan) (Maeda *et al.*, 2008b). The CCR5 inhibitor MVC was kindly provided by Pfizer (Groton, CT, USA).

Flow cytometric analysis. PM1 and PM1/CCR5 cells were analysed for surface expression of CCR5 and CXCR4. The cells (5×10^5) were incubated with phycoerythrin-labelled anti-CCR5 mAb 2D7, phycoerythrin-labelled anti-CXCR4 mAb 12G5 or isotype-matched control mAbs (BD Biosciences) and analysed using a FACSCalibur (Becton Dickinson).

***In vitro* selection of HIV-1 variants using anti-HIV drugs.** HIV-1_{KP-5} was infected into PM1/CCR5 cells and treated with various concentrations of MVC to induce the production of MVC-resistant variants as described previously (Harada *et al.*, 2013; Hatada *et al.*, 2010; Yoshimura *et al.*, 2006, 2010), with minor modifications. Briefly, PM1/CCR5 cells (4×10^4) were exposed to 500 $TCID_{50}$ HIV-1_{KP-5} and cultured in the presence of MVC. The culture supernatant was harvested on day 7 and used to infect fresh PM1/CCR5 cells for the next round of culture in the presence of increasing concentrations of MVC. We also passaged the virus in the absence of MVC in PM1/CCR5 cells and the parental cell line PM1. Proviral DNA was extracted from lysates of infected cells at different passages and subjected to nucleotide sequencing.

Amplification of proviral DNA and nucleotide sequencing. Proviral DNA was subjected to PCR amplification using PrimeSTAR GXL DNA polymerase and Ex-*Taq* polymerase (Takara) as described previously (Harada *et al.*, 2013; Hatada *et al.*, 2010; Yoshimura *et al.*, 2006, 2010). Primers 1B and H were used for the gp120 region (Harada *et al.*, 2013; Hatada *et al.*, 2010). The first-round PCR products were used directly in a second round of PCR using primers 2B and F for gp120 (Harada *et al.*, 2013; Hatada *et al.*, 2010). The second-round PCR products were purified and cloned into the pGEM-T Easy Vector (Promega), and the *env* region in each passaged virus was sequenced using a 3500xL Genetic Analyzer (Applied Biosystems).

Susceptibility assay. The sensitivities of the passaged viruses to various drugs were determined as described previously (Harada *et al.*, 2013; Hatada *et al.*, 2010; Yoshimura *et al.*, 2006, 2010), with minor modifications. Briefly, PM1/CCR5 cells were plated in 96-well round-bottom plates (2×10^3 cells per well), exposed to 100 $TCID_{50}$ of the viruses in the presence of various concentrations of drugs and incubated at 37 °C for 7 days. The IC_{50} values were then determined using a Cell Counting kit-8 (WST-8 assay; Dojindo Laboratories). All assays were performed in duplicate or triplicate.

PHA-activated PBMCs (1×10^6 cells ml^{-1}) were exposed to 100 $TCID_{50}$ of each HIV-1 strain and cultured in the presence or absence of various concentrations of drugs in 96-well microculture plates. The concentration of p24 antigen produced by the cells was determined on day 7 using a Lumipulse F system (Fujirebio) (Maeda *et al.*, 2001). IC_{50} values were determined by comparison with the p24 production level in drug-free control cell cultures (Shirasaka *et al.*, 1995). All assays were performed in triplicate.

Construction of chimeric NL4-3/KP-5 *env* proviruses. Chimeric proviruses were constructed from the pNL4-3 proviral plasmid (ARRRP) by overlapping PCR as described previously (Shibata *et al.*, 2007), with minor modifications. Briefly, the gp160 coding sequences were amplified from the cloning vectors using the primers EnvFv (5′-AGCAGAAGACAGTGGCAATGAGAGCGAAG-3′) and EnvR (5′-TTTTGACCACTTGCCACCCATCTTATAGC-3′). A portion of the NL4-3 provirus spanning nt 5284–6232 was amplified with primers NL(5284)F (5′-GGTCAGGGAGTCTCCATAGAATGGAGG-3′) and NL(6232)Rv (5′-CTTCGCTCTCATTGCCACTGTCTTCTGCT-3′). This fragment encompasses the unique *Eco*RI restriction site in pNL4-3. Another fragment from the NL4-3 provirus spanning nt 8779–9045 was amplified using the primers NL(8779)F (5-GCTATAAGATGGGTGGCAAGTGGTCAAAA-3) and NL(9045)R (5-GATCTACAGCTGCCTTGTAAGTCATTGGTC-3). This fragment includes the unique *Xho*I restriction site in pNL4-3. Overlapping PCR was used to join the gp160 coding sequence from the desired clone to the fragment encompassing nt 8779–9045 that had been amplified from pNL4-3. The resulting fragment was then similarly joined to the amplified fragment encompassing nt 5284–6232 from pNL4-3.

The sensitivities of the three infectious clones to KD-247 (anti-V3 mAb) (Eda *et al.*, 2006), b12 (anti-CD4bs mAb; kindly provided by

Dr Dennis Burton, Scripps Research Institute, La Jolla, CA) (Kessler *et al.*, 1997), 4E9C (anti-CD4i mAb) (Yoshimura *et al.*, 2010) and autologous plasma IgGs were also determined by the WST-8 assay. Plasma samples were collected from the patient seven times from January 2010 to April 2011 and purified using Protein A Sepharose Fast Flow (GE Healthcare) (Kimura *et al.*, 2002; Yoshimura *et al.*, 2010). The purified plasma IgGs were designated KP-5-IgG-1 to KP-5-IgG-7.

Crystal structure of gp120. To compare the sequences of the MVC-selected and low-CCR5-adapted variants in 3D space, the crystal structures of the gp120 monomer and trimer were obtained from the PDB (IDs: 2B4C and 3J5M). Figures were generated using ViewerLite version 5.0 (Accelrys).

ACKNOWLEDGEMENTS

We thank The Chemo-Sero-Therapeutic Research Institute for kindly providing mAb KD-247. We also thank Dr Dennis Burton for kindly providing mAb b12. We are grateful to Dr Yosuke Maeda for providing the PM1/CCR5 cells. We also thank Aki Yamaguchi, Akiko Honda-Shibata and Noriko Shirai for excellent technical assistance. We greatly thank Dr Mark de Souza for his English proofreading. This work was supported in part by the Ministry of Health, Labour and Welfare of Japan (H22-RPEDMD-G-007 to S. M. and K. Y.; H23-AIDS-G-001, H24-AIDS-G-006 and H25-G-006 to K. Y.), the Ministry of Education, Culture, Sports, Science and Technology of Japan (24591485 and 23590548 to K. Y.; 24590199 to S. H.), and the Cooperative Research Project on Clinical and Epidemiological Studies of Emerging and Re-emerging Infectious Diseases and the Global COE Program (Global Education and Research Centre Aiming at the Control of AIDS), MEXT, Japan.

REFERENCES

Anastassopoulou, C. G., Ketas, T. J., Klasse, P. J. & Moore, J. P. (2009). Resistance to CCR5 inhibitors caused by sequence changes in the fusion peptide of HIV-1 gp41. *Proc Natl Acad Sci U S A* **106**, 5318–5323.

Berger, E. A., Murphy, P. M. & Farber, J. M. (1999). Chemokine receptors as HIV-1 coreceptors: roles in viral entry, tropism, and disease. *Annu Rev Immunol* **17**, 657–700.

Berro, R., Sanders, R. W., Lu, M., Klasse, P. J. & Moore, J. P. (2009). Two HIV-1 variants resistant to small molecule CCR5 inhibitors differ in how they use CCR5 for entry. *PLoS Pathog* **5**, e1000548.

Brelot, A., Heveker, N., Adema, K., Hosie, M. J., Willett, B. & Alizon, M. (1999). Effect of mutations in the second extracellular loop of CXCR4 on its utilization by human and feline immunodeficiency viruses. *J Virol* **73**, 2576–2586.

Cormier, E. G. & Dragic, T. (2002). The crown and stem of the V3 loop play distinct roles in human immunodeficiency virus type 1 envelope glycoprotein interactions with the CCR5 coreceptor. *J Virol* **76**, 8953–8957.

Dorr, P., Westby, M., Dobbs, S., Griffin, P., Irvine, B., Macartney, M., Mori, J., Rickett, G., Smith-Burchnell, C. & other authors (2005). Maraviroc (UK-427,857), a potent, orally bioavailable, and selective small-molecule inhibitor of chemokine receptor CCR5 with broad-spectrum anti-human immunodeficiency virus type 1 activity. *Antimicrob Agents Chemother* **49**, 4721–4732.

Dragic, T., Trkola, A., Thompson, D. A., Cormier, E. G., Kajumo, F. A., Maxwell, E., Lin, S. W., Ying, W., Smith, S. O. & other authors (2000). A binding pocket for a small molecule inhibitor of HIV-1 entry within the transmembrane helices of CCR5. *Proc Natl Acad Sci U S A* **97**, 5639–5644.

Eda, Y., Takizawa, M., Murakami, T., Maeda, H., Kimachi, K., Yonemura, H., Koyanagi, S., Shiosaki, K., Higuchi, H. & other authors (2006). Sequential immunization with V3 peptides from primary human immunodeficiency virus type 1 produces cross-neutralizing antibodies against primary isolates with a matching narrow-neutralization sequence motif. *J Virol* **80**, 5552–5562.

Farzan, M., Mirzabekov, T., Kolchinsky, P., Wyatt, R., Cayabyab, M., Gerard, N. P., Gerard, C., Sodroski, J. & Choe, H. (1999). Tyrosine sulfation of the amino terminus of CCR5 facilitates HIV-1 entry. *Cell* **96**, 667–676.

Fätkenheuer, G., Nelson, M., Lazzarin, A., Konourina, I., Hoepelman, A. I., Lampiris, H., Hirschel, B., Tebas, P., Raffi, F. & other authors (2008). Subgroup analyses of maraviroc in previously treated R5 HIV-1 infection. *N Engl J Med* **359**, 1442–1455.

Gulick, R. M., Lalezari, J., Goodrich, J., Clumeck, N., DeJesus, E., Horban, A., Nadler, J., Clotet, B., Karlsson, A. & other authors (2008). Maraviroc for previously treated patients with R5 HIV-1 infection. *N Engl J Med* **359**, 1429–1441.

Guttman, M., Kahn, M., Garcia, N. K., Hu, S. L. & Lee, K. K. (2012). Solution structure, conformational dynamics, and CD4-induced activation in full-length, glycosylated, monomeric HIV gp120. *J Virol* **86**, 8750–8764.

Harada, S., Yoshimura, K., Yamaguchi, A., Boonchawalit, S., Yusa, K. & Matsushita, S. (2013). Impact of antiretroviral pressure on selection of primary human immunodeficiency virus type 1 envelope sequences *in vitro*. *J Gen Virol* **94**, 933–943.

Hatada, M., Yoshimura, K., Harada, S., Kawanami, Y., Shibata, J. & Matsushita, S. (2010). Human immunodeficiency virus type 1 evasion of a neutralizing anti-V3 antibody involves acquisition of a potential glycosylation site in V2. *J Gen Virol* **91**, 1335–1345.

Henrich, T. J., Tsibris, A. M., Lewine, N. R., Konstantinidis, I., Leopold, K. E., Sagar, M. & Kuritzkes, D. R. (2010). Evolution of CCR5 Antagonist Resistance in an HIV-1 Subtype C Clinical Isolate. *J Acquir Immune Defic Syndr* **55**, 420–427.

Huang, C. C., Tang, M., Zhang, M. Y., Majeed, S., Montabana, E., Stanfield, R. L., Dimitrov, D. S., Korber, B., Sodroski, J. & other authors (2005). Structure of a V3-containing HIV-1 gp120 core. *Science* **310**, 1025–1028.

Kessler, J. A., II, McKenna, P. M., Emini, E. A., Chan, C. P., Patel, M. D., Gupta, S. K., Mark, G. E., III, Barbas, C. F., III, Burton, D. R. & Conley, A. J. (1997). Recombinant human monoclonal antibody IgG1b12 neutralizes diverse human immunodeficiency virus type 1 primary isolates. *AIDS Res Hum Retroviruses* **13**, 575–582.

Kimura, T., Yoshimura, K., Nishihara, K., Maeda, Y., Matsumi, S., Koito, A. & Matsushita, S. (2002). Reconstitution of spontaneous neutralizing antibody response against autologous human immunodeficiency virus during highly active antiretroviral therapy. *J Infect Dis* **185**, 53–60.

Kuhmann, S. E., Pugach, P., Kunstman, K. J., Taylor, J., Stanfield, R. L., Snyder, A., Strizki, J. M., Riley, J., Baroudy, B. M. & other authors (2004). Genetic and phenotypic analyses of human immunodeficiency virus type 1 escape from a small-molecule CCR5 inhibitor. *J Virol* **78**, 2790–2807.

Landovitz, R. J., Angel, J. B., Hoffmann, C., Horst, H., Opravil, M., Long, J., Greaves, W. & Fätkenheuer, G. (2008). Phase II study of vicriviroc versus efavirenz (both with zidovudine/lamivudine) in treatment-naive subjects with HIV-1 infection. *J Infect Dis* **198**, 1113–1122.

Lusso, P., Cocchi, F., Balotta, C., Markham, P. D., Louie, A., Farci, P., Pal, R., Gallo, R. C. & Reitz, M. S., Jr (1995). Growth of macrophage-tropic and primary human immunodeficiency virus type 1 (HIV-1)

isolates in a unique CD4$^+$ T-cell clone (PM1): failure to down-regulate CD4 and to interfere with cell-line-tropic HIV-1. *J Virol* **69**, 3712–3720.

Lyumkis, D., Julien, J. P., de Val, N., Cupo, A., Potter, C. S., Klasse, P. J., Burton, D. R., Sanders, R. W., Moore, J. P. & other authors (2013). Cryo-EM structure of a fully glycosylated soluble cleaved HIV-1 envelope trimer. *Science* **342**, 1484–1490.

Maeda, K., Yoshimura, K., Shibayama, S., Habashita, H., Tada, H., Sagawa, K., Miyakawa, T., Aoki, M., Fukushima, D. & Mitsuya, H. (2001). Novel low molecular weight spirodiketopiperazine derivatives potently inhibit R5 HIV-1 infection through their antagonistic effects on CCR5. *J Biol Chem* **276**, 35194–35200.

Maeda, K., Das, D., Ogata-Aoki, H., Nakata, H., Miyakawa, T., Tojo, Y., Norman, R., Takaoka, Y., Ding, J. & other authors (2006). Structural and molecular interactions of CCR5 inhibitors with CCR5. *J Biol Chem* **281**, 12688–12698.

Maeda, K., Das, D., Yin, P. D., Tsuchiya, K., Ogata-Aoki, H., Nakata, H., Norman, R. B., Hackney, L. A., Takaoka, Y. & Mitsuya, H. (2008a). Involvement of the second extracellular loop and transmembrane residues of CCR5 in inhibitor binding and HIV-1 fusion: insights into the mechanism of allosteric inhibition. *J Mol Biol* **381**, 956–974.

Maeda, Y., Yusa, K. & Harada, S. (2008b). Altered sensitivity of an R5X4 HIV-1 strain 89.6 to coreceptor inhibitors by a single amino acid substitution in the V3 region of gp120. *Antiviral Res* **77**, 128–135.

Marozsan, A. J., Kuhmann, S. E., Morgan, T., Herrera, C., Rivera-Troche, E., Xu, S., Baroudy, B. M., Strizki, J. & Moore, J. P. (2005). Generation and properties of a human immunodeficiency virus type 1 isolate resistant to the small molecule CCR5 inhibitor, SCH-417690 (SCH-D). *Virology* **338**, 182–199.

Ogert, R. A., Wojcik, L., Buontempo, C., Ba, L., Buontempo, P., Ralston, R., Strizki, J. & Howe, J. A. (2008). Mapping resistance to the CCR5 co-receptor antagonist vicriviroc using heterologous chimeric HIV-1 envelope genes reveals key determinants in the C2-V5 domain of gp120. *Virology* **373**, 387–399.

Ogert, R. A., Ba, L., Hou, Y., Buontempo, C., Qiu, P., Duca, J., Murgolo, N., Buontempo, P., Ralston, R. & Howe, J. A. (2009). Structure–function analysis of human immunodeficiency virus type 1 gp120 amino acid mutations associated with resistance to the CCR5 coreceptor antagonist vicriviroc. *J Virol* **83**, 12151–12163.

Ogert, R. A., Hou, Y., Ba, L., Wojcik, L., Qiu, P., Murgolo, N., Duca, J., Dunkle, L. M., Ralston, R. & Howe, J. A. (2010). Clinical resistance to vicriviroc through adaptive V3 loop mutations in HIV-1 subtype D gp120 that alter interactions with the N-terminus and ECL2 of CCR5. *Virology* **400**, 145–155.

Pantophlet, R. & Burton, D. R. (2006). GP120: target for neutralizing HIV-1 antibodies. *Annu Rev Immunol* **24**, 739–769.

Pugach, P., Marozsan, A. J., Ketas, T. J., Landes, E. L., Moore, J. P. & Kuhmann, S. E. (2007). HIV-1 clones resistant to a small molecule CCR5 inhibitor use the inhibitor-bound form of CCR5 for entry. *Virology* **361**, 212–228.

Ratcliff, A. N., Shi, W. & Arts, E. J. (2013). HIV-1 resistance to maraviroc conferred by a CD4 binding site mutation in the envelope glycoprotein gp120. *J Virol* **87**, 923–934.

Roche, M., Jakobsen, M. R., Ellett, A., Salimiseyedabad, H., Jubb, B., Westby, M., Lee, B., Lewin, S. R., Churchill, M. J. & Gorry, P. R. (2011a). HIV-1 predisposed to acquiring resistance to maraviroc (MVC) and other CCR5 antagonists *in vitro* has an inherent, low-level ability to utilize MVC-bound CCR5 for entry. *Retrovirology* **8**, 89.

Roche, M., Jakobsen, M. R., Sterjovski, J., Ellett, A., Posta, F., Lee, B., Jubb, B., Westby, M., Lewin, S. R. & other authors (2011b). HIV-1 escape from the CCR5 antagonist maraviroc associated with an altered and less-efficient mechanism of gp120–CCR5 engagement that attenuates macrophage tropism. *J Virol* **85**, 4330–4342.

Shibata, J., Yoshimura, K., Honda, A., Koito, A., Murakami, T. & Matsushita, S. (2007). Impact of V2 mutations on escape from a potent neutralizing anti-V3 monoclonal antibody during *in vitro* selection of a primary human immunodeficiency virus type 1 isolate. *J Virol* **81**, 3757–3768.

Shirasaka, T., Kavlick, M. F., Ueno, T., Gao, W. Y., Kojima, E., Alcaide, M. L., Chokekijchai, S., Roy, B. M., Arnold, E. & Yarchoan, R. (1995). Emergence of human immunodeficiency virus type 1 variants with resistance to multiple dideoxynucleosides in patients receiving therapy with dideoxynucleosides. *Proc Natl Acad Sci U S A* **92**, 2398–2402.

Tilton, J. C., Wilen, C. B., Didigu, C. A., Sinha, R., Harrison, J. E., Agrawal-Gamse, C., Henning, E. A., Bushman, F. D., Martin, J. N. & other authors (2010). A maraviroc-resistant HIV-1 with narrow cross-resistance to other CCR5 antagonists depends on both N-terminal and extracellular loop domains of drug-bound CCR5. *J Virol* **84**, 10863–10876.

Tsamis, F., Gavrilov, S., Kajumo, F., Seibert, C., Kuhmann, S., Ketas, T., Trkola, A., Palani, A., Clader, J. W. & other authors (2003). Analysis of the mechanism by which the small-molecule CCR5 antagonists SCH-351125 and SCH-350581 inhibit human immunodeficiency virus type 1 entry. *J Virol* **77**, 5201–5208.

Tsibris, A. M., Sagar, M., Gulick, R. M., Su, Z., Hughes, M., Greaves, W., Subramanian, M., Flexner, C., Giguel, F. & other authors (2008). *In vivo* emergence of vicriviroc resistance in a human immunodeficiency virus type 1 subtype C-infected subject. *J Virol* **82**, 8210–8214.

Westby, M., Lewis, M., Whitcomb, J., Youle, M., Pozniak, A. L., James, I. T., Jenkins, T. M., Perros, M. & van der Ryst, E. (2006). Emergence of CXCR4-using human immunodeficiency virus type 1 (HIV-1) variants in a minority of HIV-1-infected patients following treatment with the CCR5 antagonist maraviroc is from a pretreatment CXCR4-using virus reservoir. *J Virol* **80**, 4909–4920.

Westby, M., Smith-Burchnell, C., Mori, J., Lewis, M., Mosley, M., Stockdale, M., Dorr, P., Ciaramella, G. & Perros, M. (2007). Reduced maximal inhibition in phenotypic susceptibility assays indicates that viral strains resistant to the CCR5 antagonist maraviroc utilize inhibitor-bound receptor for entry. *J Virol* **81**, 2359–2371.

Wyatt, R. & Sodroski, J. (1998). The HIV-1 envelope glycoproteins: fusogens, antigens, and immunogens. *Science* **280**, 1884–1888.

Yoshimura, K., Shibata, J., Kimura, T., Honda, A., Maeda, Y., Koito, A., Murakami, T., Mitsuya, H. & Matsushita, S. (2006). Resistance profile of a neutralizing anti-HIV monoclonal antibody, KD-247, that shows favourable synergism with anti-CCR5 inhibitors. *AIDS* **20**, 2065–2073.

Yoshimura, K., Harada, S., Shibata, J., Hatada, M., Yamada, Y., Ochiai, C., Tamamura, H. & Matsushita, S. (2010). Enhanced exposure of human immunodeficiency virus type 1 primary isolate neutralization epitopes through binding of CD4 mimetic compounds. *J Virol* **84**, 7558–7568.

Yuan, Y., Maeda, Y., Terasawa, H., Monde, K., Harada, S. & Yusa, K. (2011). A combination of polymorphic mutations in V3 loop of HIV-1 gp120 can confer noncompetitive resistance to maraviroc. *Virology* **413**, 293–299.

Yusa, K., Maeda, Y., Fujioka, A., Monde, K. & Harada, S. (2005). Isolation of TAK-779-resistant HIV-1 from an R5 HIV-1 GP120 V3 loop library. *J Biol Chem* **280**, 30083–30090.

JVI
Journals.ASM.org

Tertiary Mutations Stabilize CD8$^+$ T Lymphocyte Escape-Associated Compensatory Mutations following Transmission of Simian Immunodeficiency Virus

Benjamin J. Burwitz,[a,b] Helen L. Wu,[a,g] Jason S. Reed,[a] Katherine B. Hammond,[a] Laura P. Newman,[d] Benjamin N. Bimber,[b] Francesca A. Nimiyongskul,[d] Enrique J. Leon,[a] Nicholas J. Maness,[c] Thomas C. Friedrich,[e,f] Masaru Yokoyama,[h] Hironori Sato,[h] Tetsuro Matano,[i] David H. O'Connor,[d,e] Jonah B. Sacha[a,b,g]

Vaccine & Gene Therapy Institute[a] and Division of Pathobiology and Immunology, Oregon National Primate Research Center,[b] Oregon Health & Science University, Portland, Oregon, USA; Division of Microbiology, Tulane National Primate Research Center, Covington, Louisiana, USA[c]; Department of Pathology, University of Wisconsin—Madison, Madison, Wisconsin, USA[d]; Wisconsin National Primate Research Center, Madison, Wisconsin, USA[e]; Department of Pathobiological Sciences, University of Wisconsin School of Veterinary Medicine, Madison, Wisconsin, USA[f]; Molecular Microbiology & Immunology, Oregon Health & Science University, Portland, Oregon, USA[g]; Laboratory of Viral Genomics, Pathogen Genomics Center, National Institute of Infectious Diseases, Musashi Murayama-shi, Tokyo, Japan[h]; AIDS Research Center, National Institute of Infectious Diseases, Shinjuku, Tokyo, Japan[i]

Compensatory mutations offset fitness defects resulting from CD8$^+$ T lymphocyte ($CD8_{TL}$)-mediated escape, but their impact on viral evolution following transmission to naive hosts remains unclear. Here, we investigated the reversion kinetics of $Gag_{181-189}$CM9 $CD8_{TL}$ escape-associated compensatory mutations in simian immunodeficiency virus (SIV)-infected macaques. Preexisting compensatory mutations did not result in acute-phase escape of the SIVmac239 CD8TL epitope Gag181-189CM9 and instead required a tertiary mutation for stabilization in the absence of $Gag_{181-189}$CM9 escape mutations. Therefore, transmitted compensatory mutations do not necessarily predict rapid $CD8_{TL}$ escape.

Reversion of particular CD8$^+$ T lymphocyte ($CD8_{TL}$) escape mutations is well documented following human immunodeficiency virus (HIV) transmission between HLA-discordant individuals and is dependent upon the fitness cost of the escape mutation. Escape mutations that exact a high fitness cost often revert following HIV transmission to an HLA-discordant individual, while those that impose a low fitness cost do not (1–3). Two epitopes targeted by $CD8_{TL}$ responses associated with long-term HIV control, HLA-B*27-bound $Gag_{263-272}$KK10 and HLA-B*57-bound $Gag_{240-249}$TW10, lie within a conserved region of Gag, and escape mutations within these epitopes reduce viral fitness. However, while the codon 242 threonine-to-asparagine ($T_{242}N$) escape mutation within $Gag_{240-249}$TW10 reverts readily following transmission to an HLA-disparate host, the $R_{264}K$ escape mutation within $Gag_{263-272}$KK10 does not (3, 4). This finding is surprising given that the $R_{264}K$ mutation reduces viral replicative fitness to a significantly greater extent than the $T_{242}N$ mutation (5). Compensatory mutations that maintain viral fitness while allowing for intra-epitopic variation have been described for both $Gag_{263-272}$KK10 and $Gag_{240-249}$TW10, and the difference in reversion kinetics between these epitopes is likely dependent on these compensatory mutations (4, 6, 7).

In simian immunodeficiency virus mac239 (SIVmac239)-infected rhesus macaques, the Mamu-A1*001:01-bound $CD8_{TL}$ epitope $Gag_{181-189}$CM9 is analogous to $Gag_{263-272}$KK10 and $Gag_{240-249}$TW10 in that it lies within a conserved region of Gag and has associated compensatory mutations that increase the fitness of viral variants containing $Gag_{181-189}$CM9 escape mutations. We, and others, have previously shown that the canonical $Gag_{181-189}$CM9 escape mutation $T_{182}A$ is frequently linked with the flanking downstream mutation $I_{206}V$ and reverts following transmission to *Mamu-A1*001:01*-negative rhesus macaques (8–10). Additionally, the $I_{206}V$ compensatory mutation is consistently associated with a subsequent upstream mutation, $I_{161}V$. This mutation is not necessary for the emergence of viruses with the $T_{182}A$ escape mutation, but it is believed to further increase viral fitness following mutations at both T_{182} and I_{206}.

We hypothesized that preexisting $I_{161}V$ and $I_{206}V$ compensatory mutations would facilitate rapid, acute-phase escape within the conserved $Gag_{181-189}$CM9 $CD8_{TL}$ epitope upon transmission to *Mamu-A1*001:01*-positive rhesus macaques. To test this hypothesis, we engineered an SIVmac239 variant harboring the $I_{161}V$ and $I_{206}V$ compensatory mutations associated with $Gag_{181-189}$CM9 escape (SIVmac239-2V) by site-directed mutagenesis of SIVmac239 plasmid DNA using the QuikChange XL kit (Stratagene, La Jolla, CA) and generated a virus stock as previously described (2). Following intravenous infection of a *Mamu-A1*001:01*-positive rhesus macaque, r98003, with 100 ng Gag $p27^{CA}$, SIVmac239-2V replicated efficiently, peaking at 3.96×10^7 viral RNA (vRNA) copies/ml plasma at 10 days postinfection (d.p.i.), as measured by quantitative reverse transcription-PCR (RT-PCR) using previously described techniques (11) (Fig. 1A). This level of viral replication is consistent with a large body of data collected from wild-type SIVmac239-infected *Mamu-A1*001:01*-positive rhesus macaques (12, 13). Additionally, major histocompatibility complex (MHC) class I tetramer staining of freshly isolated peripheral blood mononuclear cells (PBMC) revealed that SIVmac239-2V elicited a strong $CD8_{TL}$ response against $Gag_{181-189}$CM9, with 3.5% of all circulating $CD8_{TL}$ tar-

Received 12 November 2013 **Accepted** 22 December 2013
Published ahead of print 26 December 2013
Editor: G. Silvestri
Address correspondence and reprint requests to Jonah B. Sacha, sacha@ohsu.edu.
B.J.B. and H.L.W. contributed equally to this work.

doi:10.1128/JVI.03304-13

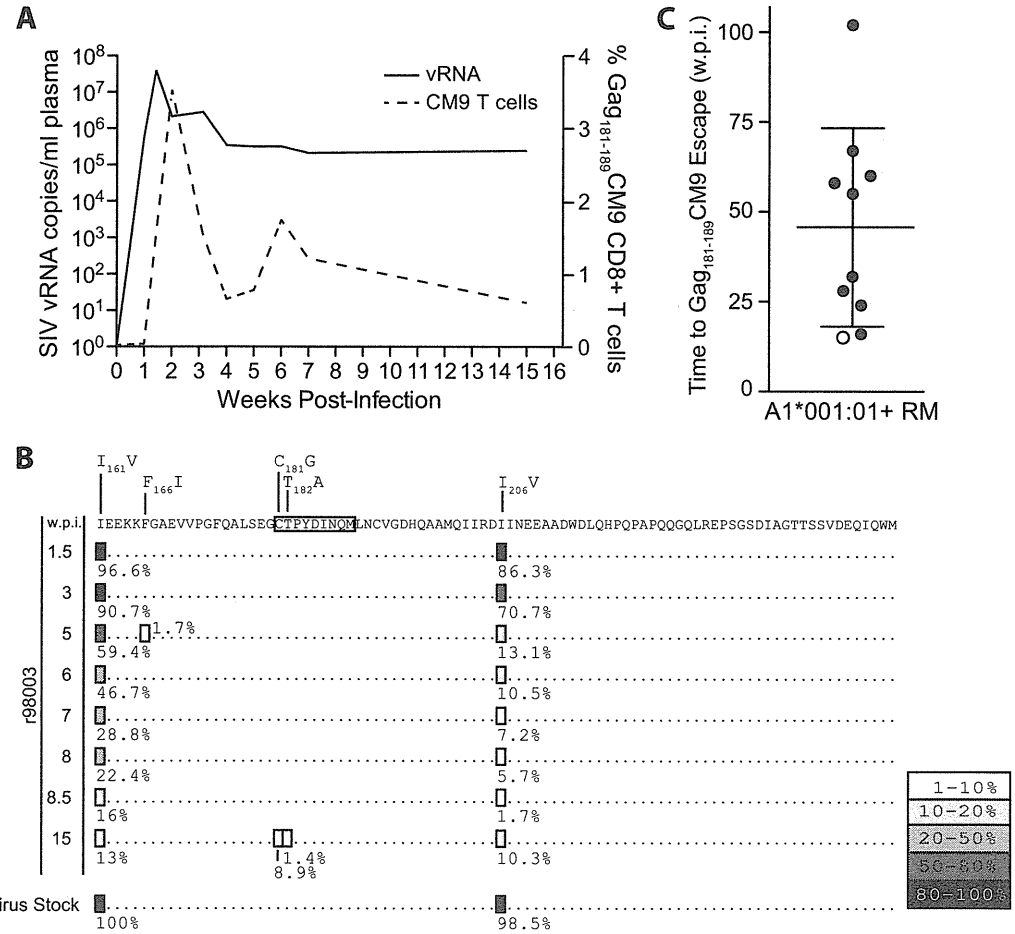

FIG 1 Compensatory mutations in SIVmac239-2V revert rapidly to wild type despite a $Gag_{181-189}$CM9-specific $CD8_{TL}$ response. (A) Replication of the engineered SIVmac239 mutant SIVmac239-2V in r98003 was monitored in plasma over the first 15 weeks postinfection (w.p.i.). During the same period, the magnitude of the $Gag_{181-189}$CM9-specific $CD8_{TL}$ response was assessed by Mamu-A1*001:01/$Gag_{181-189}$CM9 tetramer staining. (B) The $Gag_{181-189}$CM9 region from the SIVmac239-2V-infected, *Mamu-A1*00101*-positive rhesus macaque r98003 was Roche/454 pyrosequenced at the indicated w.p.i. Each consensus sequence indicates all mutations present in 1% or more of total sequence reads (limit of detection). Amino acid substitutions are shown above the reference sequence; the frequencies of the mutations are shown both as percentages and as shaded boxes according to prevalence, as indicated by the key at the bottom right. Boxed amino acids within the reference sequence comprise the $Gag_{181-189}$CM9 epitope. The consensus sequence of the SIVmac239-2V virus stock used to infect r98003 is shown below the sequences from r98003. (C) Times to $Gag_{181-189}$CM9 escape (as defined by the first of two consecutive time points showing amino acid substitutions within the epitope at a frequency of >1% of total sequence reads) in nine *Mamu-A1*00101*-positive rhesus macaques (filled circles) and animal r98003 (open circle). The means and standard deviations of times to $Gag_{181-189}$CM9 escape are shown.

geting this epitope at 14 d.p.i. (Fig. 1A). Importantly, this $Gag_{181-189}$CM9-specific $CD8_{TL}$ response remained at high frequency in r98003 through 15 weeks p.i. (w.p.i.).

Next, we monitored viral evolution within *gag* by performing Roche/454 pyrosequencing on plasma samples as described previously (8). Unexpectedly, instead of observing rapid, acute-phase escape of $Gag_{181-189}$CM9, we detected high-frequency reversions of both the $I_{161}V$ and $I_{206}V$ compensatory mutations (Fig. 1B). The frequency of revertant viruses in plasma increased through 8.5 w.p.i., when 98.3% of plasma virus sequences were wild-type SIVmac239 at I_{206} and 84% were wild-type SIVmac239 at I_{161}. Subsequently, we detected two $Gag_{181-189}$CM9 escape mutations, $C_{181}G$ and $T_{182}A$, only after the $I_{206}V$ compensatory mutation had reverted almost entirely to wild type, with $I_{206}V$ present in only 1.7% of all pyrosequencing reads (Fig. 1B). The $C_{181}G$ mutation is rare but is a previously described $Gag_{181-189}$CM9 escape mutation that also associates with the $I_{161}V$ and $I_{206}V$ compensatory mutations in *Mamu-A1*001:01*-positive, SIVmac239-infected rhesus macaques (8, 9). These three mutations increased in frequency together and were tightly linked, with 87% of sequences containing one or both escape mutations also harboring the $I_{206}V$ compensatory mutation (data not shown). While we failed to observe rapid acute-phase $CD8_{TL}$ escape, r98003 did manifest the earliest Gag181-189CM9 escape mutations of nine *Mamu-A1*001:01*-positive rhesus macaques that we have investigated previously via Roche/454 pyrosequencing (8) (Fig. 1C).

The SIV compensatory mutations Gag $I_{161}V$ and $I_{206}V$ do not always revert following transmission to *Mamu-A1*001:01*-negative rhesus macaques. Given the surprising reversion of the compensatory mutations following infection of a naive host, we next investigated additional animals infected with SIVmac239 harboring the preengineered $I_{161}V$ and $I_{206}V$ mutations. Friedrich

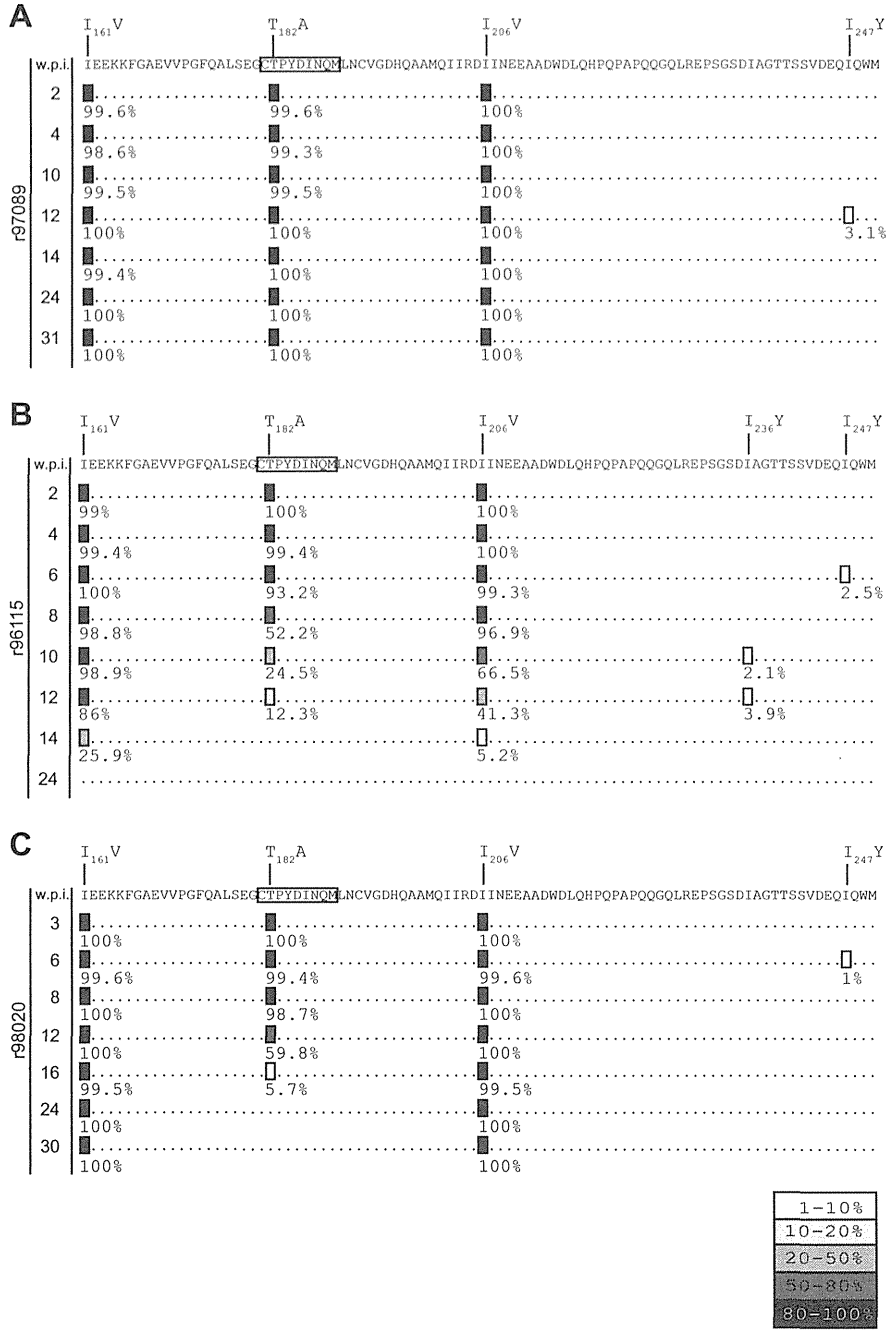

FIG 2 Consensus sequences of the $Gag_{181-189}$CM9 region in rhesus macaques infected with 3XSIVmac239. The $Gag_{181-189}$CM9 regions from three rhesus macaques infected with 3XSIVmac239 were Roche/454 pyrosequenced at the indicated w.p.i. (A) r97089 (*Mamu-A1*001:01* positive); (B) r96115 (*Mamu-A1*001:01* negative); (C) r98020 (*Mamu-A1*001:01* negative). Each consensus sequence indicates all mutations present in 1% or more of total sequence reads (limit of detection). Amino acid substitutions are shown above the reference sequence; the frequencies of the mutations are shown both as percentages and as shaded boxes according to prevalence, as indicated by the key at the bottom right. Boxed amino acids within the reference sequence comprise the $Gag_{181-189}$CM9 epitope.

et al. previously described three rhesus macaques infected with 3XSIVmac239, a virus encoding the $Gag_{181-189}$CM9 escape mutation $T_{182}A$ and the two compensatory substitutions $I_{161}V$ and $I_{206}V$ (2). We Roche/454 pyrosequenced virus from plasma samples obtained from these three animals, spanning the first 8 months of infection, to make direct comparisons with virus sequences from r98003 and to glean additional insight into why SIVmac239-2V reverted at positions $I_{161}V$ and $I_{206}V$ before $Gag_{181-189}$CM9 escape. Two of these rhesus macaques were *Mamu-A1*001:01* negative (r98020, r96115), and one was *Mamu-A1*001:01* positive (r97089). The 3XSIVmac239 circulating in r97089 retained all three ($I_{161}V$, $T_{182}A$, and $I_{206}V$) preengineered mutations, most likely due to low-frequency Mamu-A1*001:01-restricted, $Gag_{181-189}$CM9-specific $CD8_{TL}$ (14) (Fig. 2A). In con-

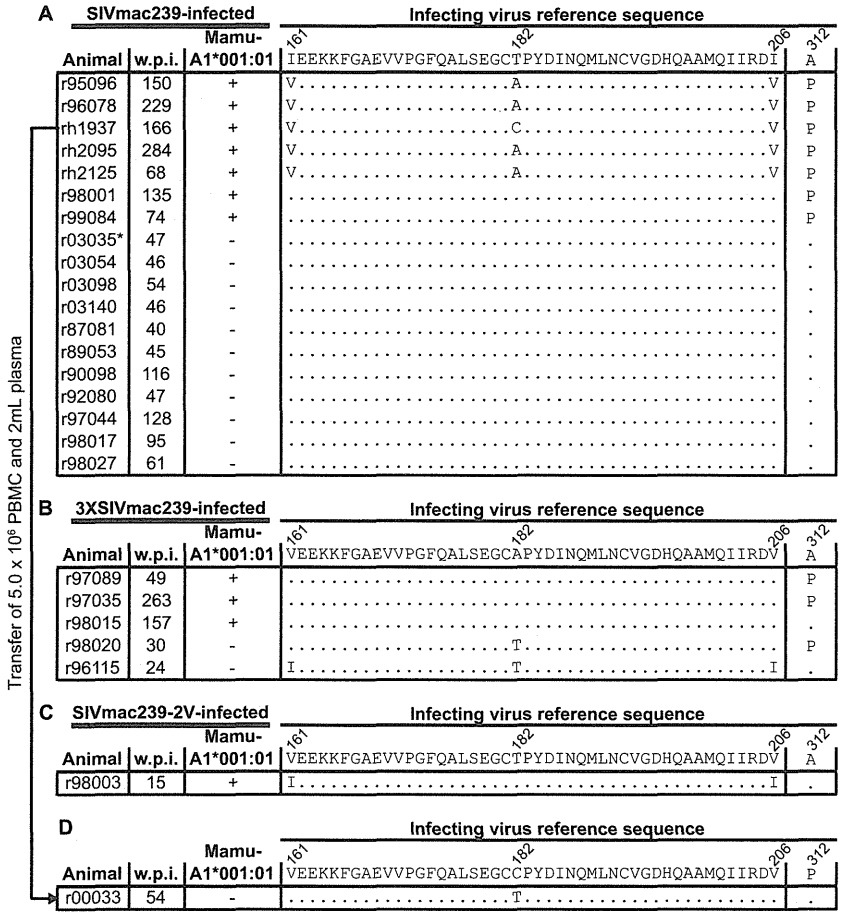

FIG 3 The Gag $A_{312}P$ mutation stabilizes the compensatory mutations Gag $I_{161}V$ and $I_{206}V$. Consensus Sanger sequences spanning Gag I_{161} through I_{206} and the tertiary mutation site Gag A_{312} at the indicated w.p.i. are shown. (A) Eighteen SIVmac239-infected rhesus macaques (seven *Mamu-A1*001:01* positive and eleven *Mamu-A1*001:01* negative). *, r03035 was infected with the SIVmac239 variant B*008:01 8 × SIVmac239 described in reference 21. (B) Five 3XSIVmac239-infected rhesus macaques (three *Mamu-A1*001:01* positive and two *Mamu-A1*001:01* negative). (C) One *Mamu-A1*001:01*-positive, SIVmac239-2V-infected rhesus macaque. (D) One *Mamu-A1*001:01*-negative rhesus macaque infected by transfer of plasma and PBMC from rh1937 at 166 w.p.i. (see the arrow). Reference sequences for respective infecting SIV strains are shown across the top.

trast, 3XSIVmac239 evolution diverged between the two *Mamu-A1*001:01*-negative animals. The 3XSIVmac239 circulating in r96115 reverted completely to wild type at all three positions (I_{161}, T_{182}, and I_{206}) by 24 w.p.i., supporting our data from r98003 (Fig. 2B). Surprisingly, 3XSIVmac239 in r98020 reverted completely to wild type at position T_{182} by 24 w.p.i. but maintained the compensatory mutations $I_{161}V$ and $I_{206}V$ in 100% of sequence reads through 30 w.p.i. (Fig. 2C). This finding is in contrast to our data from r98003 and r96115, in which compensatory mutations $I_{161}V$ and $I_{206}V$ reverted in the absence of a $Gag_{181-189}$CM9 escape mutation (Fig. 1B and 2B).

The downstream Gag mutation $A_{312}P$ stabilizes SIV containing compensatory mutations $I_{161}V$ and $I_{206}V$ in the absence of a $Gag_{181-189}$CM9 escape mutation. The divergent viral evolution between r98003, r96115, and r98020 raised the possibility that a tertiary mutation was maintaining viral fitness while allowing for the retention of the $I_{161}V$ and $I_{206}V$ compensatory mutations. To test this hypothesis, we analyzed Gag sequences from a cohort of 25 chronically SIV-infected rhesus macaques, including r98003, r97089, and r98020, at various time points postinfection (11 *Mamu-A1*001:01*-positive, 14 *Mamu-A1*001:01*-negative macaques) using consensus Sanger sequencing as previously described (15). We found that viral sequences from five of seven SIVmac239-infected, *Mamu-A1*001:01*-positive animals contained mutations $I_{161}V$, $T_{182}A/C$, $I_{206}V$, and a downstream mutation, Gag $A_{312}P$ (Fig. 3A). Virus from the two remaining *Mamu-A1*001:01*-positive animals (r98001 and r99084) harbored the $A_{312}P$ mutation alone, suggesting that this mutation can precede the $I_{161}V$, $T_{182}A/C$, and $I_{206}V$ mutations. In contrast, none of these mutations were observed in *Mamu-A1*001:01*-negative animals (Fig. 3A). Thus, it appeared that $A_{312}P$ was associated with $Gag_{181-189}$CM9 escape. Next, we examined the association of $A_{312}P$ with the maintenance of the $I_{161}V$ and $I_{206}V$ compensatory mutations following transmission of our engineered viruses to naive hosts. In two out of the three *Mamu-A1*001:01*-positive animals infected with 3XSIVmac239 (r97089 and r97035), the $A_{312}P$ mutation arose following infection, which again suggested that $A_{312}P$ stabilizes the $Gag_{181-189}$CM9 escape-associated compensatory mutations (Fig. 3B). In the two *Mamu-A1*001:01*-negative animals infected with 3XSIVmac239 (r98020 and r96115), $A_{312}P$ was present only in r98020, where the compensatory mutations persisted in the absence of $Gag_{181-189}$CM9 escape. In r98003,

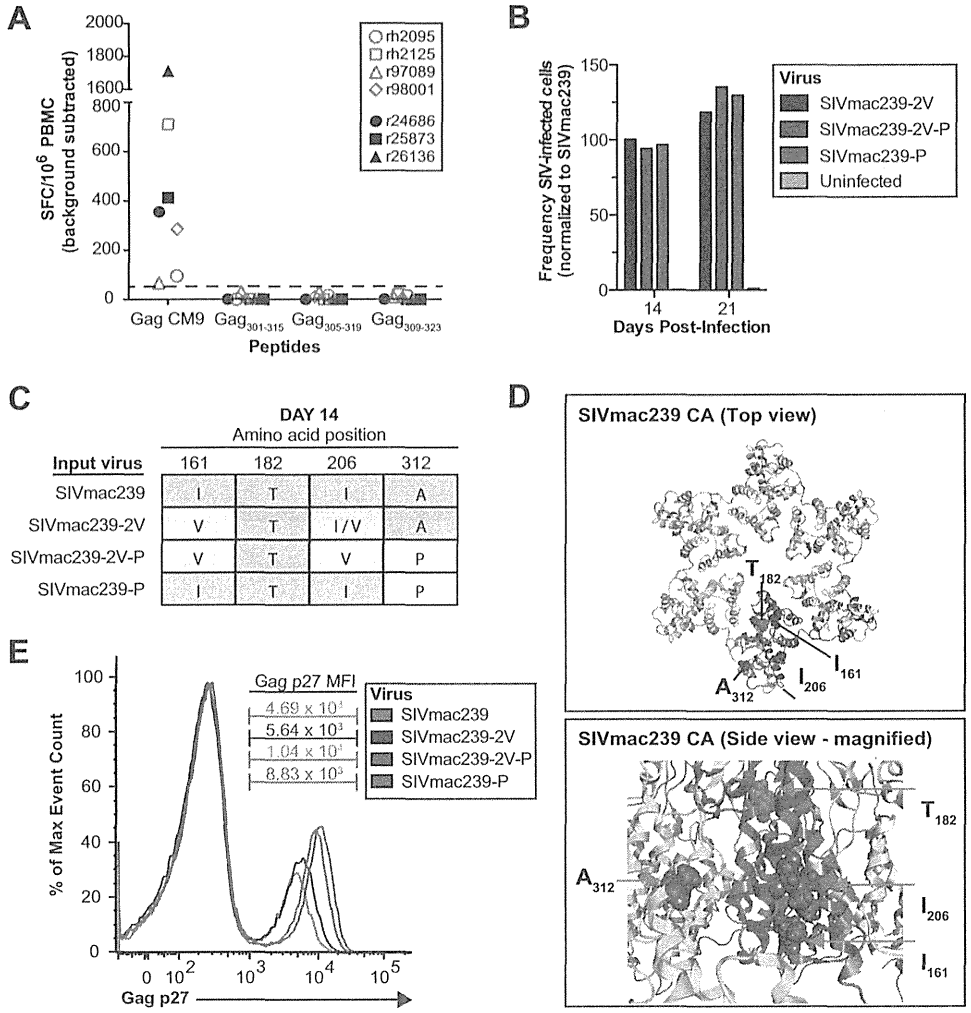

FIG 4 Gag $A_{312}P$ is a tertiary compensatory mutation stabilizing SIVmac239 CA expressing $I_{206}V$. (A) Seven *Mamu-A1*00101*-positive rhesus macaques infected with SIV were screened for T cell responses against three overlapping 15-mer peptides spanning the A_{312} region by IFN-γ ELISpot. Animals harboring SIV with the $A_{312}P$ mutation are represented with open red symbols. SFC, spot-forming cells. The dashed line at 50 SFC is the limit of detection for this assay. (B) Frequency of Gag $p27^+$ $CD4^+$ T cell targets infected with engineered mutant viruses *in vitro*. Values were normalized to the frequency of Gag $p27^+$ targets infected with SIVmac239. (C) Table showing Sanger sequencing results from vRNA taken at day 14 of the *in vitro* replication assay. (D) Structural modeling of SIVmac239 capsid, showing positions of the I_{161}, T_{182}, I_{206}, and A_{312} amino acid residues. (Top) Top view of the SIVmac239 CA hexamer, with one monomer colored light blue and a second monomer colored dark blue. (Bottom) Magnified side view of the potential interaction between A_{312} (within the light-blue monomer) and I_{206} (within the dark-blue monomer). (E) Representative Gag p27-staining histogram, showing the mean fluorescent intensity of intracellular Gag p27-fluorescein isothiocyanate (FITC) staining for each virus at day 21 of our *in vitro* replication assay. Results are indicative of separate assays performed with two different Gag p27-specific antibodies.

the *Mamu-A1*001:01*-positive animal infected with SIVmac239-2V, the lack of $A_{312}P$ was associated with reversion of the compensatory mutations to wild type (Fig. 3C).

To further test if the tertiary mutation $A_{312}P$ would stabilize the $I_{161}V$ and $I_{206}V$ compensatory mutations during reversion of $Gag_{181-189}CM9$ epitope mutations, we infected a *Mamu-A1*001:01*-negative animal, r00033, with virus from rh1937 that contained the $T_{182}C$ $Gag_{181-189}CM9$ escape mutation, the $I_{161}V$ and $I_{206}V$ compensatory mutations, and the tertiary $A_{312}P$ mutation (Fig. 3A and D). In agreement with our previous observations, the $A_{312}P$ mutation stabilized the $I_{161}V$ and $I_{206}V$ compensatory mutations, while the $T_{182}C$ escape mutation reverted to wild type (Fig. 3D). Cumulatively, these data suggest that $A_{312}P$ is necessary for the maintenance of $I_{161}V$ and $I_{206}V$ compensatory mutations in the absence of $Gag_{181-189}CM9$ escape.

Gag $A_{312}P$ is a bona fide compensatory mutation. We observed that $A_{312}P$ consistently associated with the $Gag_{181-189}CM9$ escape-associated compensatory mutations, but we wanted to further assess the compensatory characteristics of the $A_{312}P$ mutation. We first investigated the possibility that $A_{312}P$ could be a $CD8_{TL}$ escape mutation but found no evidence of T cells targeting this region of Gag. Using *in silico* binding algorithms (http://www.cbs.dtu.dk/services/NetMHC/) we found that no 8-, 9-, or 10-mer peptides between SIVmac239 Gag residues 301 and 323 are predicted to bind Mamu-A1*001:01 with physiologically relevant affinity (50% inhibitory concentration [IC_{50}] ≤ 500 nM) (16). In addition, we detected no $CD8_{TL}$ responses to the A_{312} region by a gamma interferon (IFN-γ) enzyme-linked immunosorbent spot assay (ELISpot) in 7 *Mamu-A1*001:01*-positive rhesus macaques with detectable $Gag_{181-189}CM9$-specific $CD8_{TL}$ responses, 4 of

which also had circulating virus harboring the $A_{312}P$ mutation (Fig. 4A, red symbols). These results, in combination, support the conclusion that $CD8_{TL}$ pressure does not drive the emergence of $A_{312}P$ in *Mamu-A1*001:01*-positive animals.

Next, we performed an *in vitro* SIVmac239 replication assay to compare the growth kinetics and levels of stability of viruses containing the $I_{161}V$, $I_{206}V$, and $A_{312}P$ mutations. We engineered two SIVmac239 mutants (in addition to SIVmac239-2V) containing the $I_{161}V$, $I_{206}V$, and $A_{312}P$ mutations together (SIVmac239-2V-P) or the $A_{312}P$ mutation alone (SIVmac239-P). We infected separate cultures of staphylococcal-enterotoxin B-stimulated rhesus macaque $CD4^+$ T cells with 2×10^7 virus particles of either SIVmac239 or a mutant virus in complete medium containing 100 IU interleukin 2 (IL-2)/ml and cultured them for 7 days. On days 7 and 14, virus-containing cell supernatant was diluted 1:4 with medium and used to infect additional activated $CD4^+$ T cells. We compared the frequencies of infected targets for each mutant virus on days 14 and 21 by intracellular Gag p27 antibody staining, normalizing to the frequency of SIVmac239-infected targets (Fig. 4B). Mutant viruses showed replication kinetics similar to that of SIVmac239 over the first 14 days but exhibited a higher replicative capacity by day 21. We Sanger sequenced the mutant viruses from our replication assay at day 14 and found that SIVmac239-2V, but not SIVmac239-2V-P, showed a prominent double peak indicating reversion of the $I_{206}V$ mutation (Fig. 4C).

Finally, we generated structural models of the SIVmac239 capsid (CA) hexamer as previously described (17) and assessed locations and potential interactions of the I_{161}, T_{182}, I_{206}, and A_{312} amino acid residues (Fig. 4D, top). The I_{161} residue is found in helix 1 of CA, and its side chain protrudes into helix 4, where the I_{206} residue is located, supporting the observed linkage between the $I_{161}V$ and $I_{206}V$ mutations. Importantly, the A_{312} residue lies within CA helix 9, near the I_{206}-containing helix 4 of the adjacent CA monomer (Fig. 4D, bottom). Thus, SIVmac239 CA structural data suggest that the $A_{312}P$ mutation may influence the intermolecular interactions and stability of the CA hexamer. In support of this hypothesis, we consistently detected higher levels of intracellular Gag p27 CA in cells infected with viruses containing the $A_{312}P$ mutations (Fig. 4E). Taken together, our structural and *in vitro* sequencing data strongly support our conclusion that $A_{312}P$ is a tertiary compensatory mutation that stabilizes SIVmac239 expressing the $Gag_{181-189}$CM9-associated compensatory mutation.

The association of $A_{312}P$ with the $I_{161}V$ and $I_{206}V$ compensatory mutations has not previously been described in studies of $Gag_{181-189}$CM9 escape but is not altogether an unexpected finding. In fact, the data presented herein contribute to a growing body of evidence that HIV and SIV variation within Gag is highly organized, both in terms of mutation kinetics and constrained patterns of escape (18–20). These structural restraints have contributed to the identification of Gag as a premier target for T cell-based HIV vaccine design.

As HIV circulates in human populations, there is concern that $CD8_{TL}$ epitopes will be "lost" as escape substitutions accumulate in transmitted viruses. While the finding that such escape mutations frequently revert in the absence of selecting HLA alleles ameliorates this concern, the persistence of compensatory mutations in transmitted viruses may facilitate rapid escape when the virus next encounters $CD8_{TL}$ restricted by the selecting HLA molecule. However, our data indicate that transmitted compensatory mutations do not necessarily facilitate rapid, acute-phase immune escape from $CD8_{TL}$ responses. Further study of additional compensatory mutations, in terms of their frequency in circulating HIV strains and their effect on posttransmission $CD8_{TL}$ responses, is warranted to fully understand their impact on the adaptation of HIV to HLA molecules present at high frequency within the human population.

ACKNOWLEDGMENTS

This work was supported in part by the National Center for Research Resources (grants P51 OD011092 and R21 068586).

We gratefully acknowledge David Watkins for providing longitudinal plasma and PBMC samples. We thank Anusha Hoda for technical assistance. SIVmac239 plasmids p239SpSp5′ and p239SpE3′nefopen were obtained from the NIH AIDS Reagent Program.

REFERENCES

1. **Mudd PA, Ericsen AJ, Walsh AD, Leon EJ, Wilson NA, Maness NJ, Friedrich TC, Watkins DI.** 2011. CD8+ T cell escape mutations in simian immunodeficiency virus SIVmac239 cause fitness defects in vivo, and many revert after transmission. J. Virol. **85**:12804–12810. http://dx.doi.org/10.1128/JVI.05841-11.
2. **Friedrich TC, Dodds EJ, Yant LJ, Vojnov L, Rudersdorf R, Cullen C, Evans DT, Desrosiers RC, Mothe BR, Sidney J, Sette A, Kunstman K, Wolinsky S, Piatak M, Lifson J, Hughes AL, Wilson N, O'Connor DH, Watkins DI.** 2004. Reversion of CTL escape-variant immunodeficiency viruses in vivo. Nat. Med. **10**:275–281. http://dx.doi.org/10.1038/nm998.
3. **Leslie AJ, Pfafferott KJ, Chetty P, Draenert R, Addo MM, Feeney M, Tang Y, Holmes EC, Allen T, Prado JG, Altfeld M, Brander C, Dixon C, Ramduth D, Jeena P, Thomas SA, St John A, Roach TA, Kupfer B, Luzzi G, Edwards A, Taylor G, Lyall H, Tudor-Williams G, Novelli V, Martinez-Picado J, Kiepiela P, Walker BD, Goulder PJ.** 2004. HIV evolution: CTL escape mutation and reversion after transmission. Nat. Med. **10**:282–289. http://dx.doi.org/10.1038/nm992.
4. **Schneidewind A, Brumme ZL, Brumme CJ, Power KA, Reyor LL, O'Sullivan K, Gladden A, Hempel U, Kuntzen T, Wang YE, Oniangue-Ndza C, Jessen H, Markowitz M, Rosenberg ES, Sekaly RP, Kelleher AD, Walker BD, Allen TM.** 2009. Transmission and long-term stability of compensated CD8 escape mutations. J. Virol. **83**:3993–3997. http://dx.doi.org/10.1128/JVI.01108-08.
5. **Boutwell CL, Carlson JM, Lin TH, Seese A, Power KA, Peng J, Tang Y, Brumme ZL, Heckerman D, Schneidewind A, Allen TM.** 2013. Frequent and variable cytotoxic-T-lymphocyte escape-associated fitness costs in the human immunodeficiency virus type 1 subtype B Gag proteins. J. Virol. **87**:3952–3965. http://dx.doi.org/10.1128/JVI.03233-12.
6. **Brockman MA, Brumme ZL, Brumme CJ, Miura T, Sela J, Rosato PC, Kadie CM, Carlson JM, Markle TJ, Streeck H, Kelleher AD, Markowitz M, Jessen H, Rosenberg E, Altfeld M, Harrigan PR, Heckerman D, Walker BD, Allen TM.** 2010. Early selection in Gag by protective HLA alleles contributes to reduced HIV-1 replication capacity that may be largely compensated for in chronic infection. J. Virol. **83**:11937–11949. http://dx.doi.org/10.1128/JVI.01086-10.
7. **Schneidewind A, Brockman MA, Yang R, Adam RI, Li B, Le Gall S, Rinaldo CR, Craggs SL, Allgaier RL, Power KA, Kuntzen T, Tung CS, LaBute MX, Mueller SM, Harrer T, McMichael AJ, Goulder PJ, Aiken C, Brander C, Kelleher AD, Allen TM.** 2007. Escape from the dominant HLA-B27-restricted cytotoxic T-lymphocyte response in Gag is associated with a dramatic reduction in human immunodeficiency virus type 1 replication. J. Virol. **81**:12382–12393. http://dx.doi.org/10.1128/JVI.01543-07.
8. **Burwitz BJ, Sacha JB, Reed JS, Newman LP, Norante FA, Bimber BN, Wilson NA, Watkins DI, O'Connor DH.** 2011. Pyrosequencing reveals restricted patterns of CD8+ T cell escape-associated compensatory mutations in simian immunodeficiency virus. J. Virol. **85**:13088–13096. http://dx.doi.org/10.1128/JVI.05650-11.
9. **Friedrich TC, Frye CA, Yant LJ, O'Connor DH, Kriewaldt NA, Benson M, Vojnov L, Dodds EJ, Cullen C, Rudersdorf R, Hughes AL, Wilson N, Watkins DI.** 2004. Extraepitopic compensatory substitutions partially restore fitness to simian immunodeficiency virus variants that escape from an immunodominant cytotoxic-T-lymphocyte response. J. Virol. **78**:2581–2585. http://dx.doi.org/10.1128/JVI.78.5.2581-2585.2004.

10. Peyerl FW, Barouch DH, Yeh WW, Bazick HS, Kunstman J, Kunstman KJ, Wolinsky SM, Letvin NL. 2003. Simian-human immunodeficiency virus escape from cytotoxic T-lymphocyte recognition at a structurally constrained epitope. J. Virol. 77:12572–12578. http://dx.doi.org/10.1128/JVI.77.23.12572-12578.2003.
11. Friedrich TC, Valentine LE, Yant LJ, Rakasz EG, Piaskowski SM, Furlott JR, Weisgrau KL, Burwitz B, May GE, Leon EJ, Soma T, Napoe G, Capuano SV, Wilson NA, Watkins DI. 2007. Subdominant CD8+ T-cell responses are involved in durable control of AIDS virus replication. J. Virol. 81:3465–3476. http://dx.doi.org/10.1128/JVI.02392-06.
12. Kim EY, Veazey RS, Zahn R, McEvers KJ, Baumeister SH, Foster GJ, Rett MD, Newberg MH, Kuroda MJ, Rieber EP, Piatak MJ, Lifson JD, Letvin NL, Wolinsky SM, Schmitz JE. 2008. Contribution of CD8+ T cells to containment of viral replication and emergence of mutations in Mamu-A*01-restricted epitopes in simian immunodeficiency virus-infected rhesus monkeys. J. Virol. 82:5631–5635. http://dx.doi.org/10.1128/JVI.02749-07.
13. Wilson NA, Reed J, Napoe GS, Piaskowski S, Szymanski A, Furlott J, Gonzalez EJ, Yant LJ, Maness NJ, May GE, Soma T, Reynolds MR, Rakasz E, Rudersdorf R, McDermott AB, O'Connor DH, Friedrich TC, Allison DB, Patki A, Picker LJ, Burton DR, Lin J, Huang L, Patel D, Heindecker G, Fan J, Citron M, Horton M, Wang F, Liang X, Shiver JW, Casimiro DR, Watkins DI. 2006. Vaccine-induced cellular immune responses reduce plasma viral concentrations after repeated low-dose challenge with pathogenic simian immunodeficiency virus SIVmac239. J. Virol. 80:5875–5885. http://dx.doi.org/10.1128/JVI.00171-06.
14. Friedrich TC, McDermott AB, Reynolds MR, Piaskowski S, Fuenger S, De Souza IP, Rudersdorf R, Cullen C, Yant LJ, Vojnov L, Stephany J, Martin S, O'Connor DH, Wilson N, Watkins DI. 2004. Consequences of cytotoxic T-lymphocyte escape: common escape mutations in simian immunodeficiency virus are poorly recognized in naive hosts. J. Virol. 78:10064–10073. http://dx.doi.org/10.1128/JVI.78.18.10064-10073.2004.
15. O'Connor DH, McDermott AB, Krebs KC, Dodds EJ, Miller JE, Gonzalez EJ, Jacoby TJ, Yant L, Piontkivska H, Pantophlet R, Burton DR, Rehrauer WM, Wilson N, Hughes AL, Watkins DI. 2004. A dominant role for CD8+-T-lymphocyte selection in simian immunodeficiency virus sequence variation. J. Virol. 78:14012–14022. http://dx.doi.org/10.1128/JVI.78.24.14012-14022.2004.
16. Lundegaard C, Lamberth K, Harndahl M, Buus S, Lund O, Nielsen M. 2008. NetMHC-3.0: accurate web accessible predictions of human, mouse and monkey MHC class I affinities for peptides of length 8–11. Nucleic Acids Res. 36:W509–W512. http://dx.doi.org/10.1093/nar/gkn202.
17. Inagaki N, Takeuchi H, Yokoyama M, Sato H, Ryo A, Yamamoto H, Kawada M, Matano T. 2010. A structural constraint for functional interaction between N-terminal and C-terminal domains in simian immunodeficiency virus capsid proteins. Retrovirology 7:90. http://dx.doi.org/10.1186/1742-4690-7-90.
18. Dahirel V, Shekhar K, Pereyra F, Miura T, Artyomov M, Talsania S, Allen TM, Altfeld M, Carrington M, Irvine DJ, Walker BD, Chakraborty AK. 2011. Coordinate linkage of HIV evolution reveals regions of immunological vulnerability. Proc. Natl. Acad. Sci. U. S. A. 108:11530–11535. http://dx.doi.org/10.1073/pnas.1105315108.
19. Schneidewind A, Brockman MA, Sidney J, Wang YE, Chen H, Suscovich TJ, Li B, Adam RI, Allgaier RL, Mothe BR, Kuntzen T, Oniangue-Ndza C, Trocha A, Yu XG, Brander C, Sette A, Walker BD, Allen TM. 2008. Structural and functional constraints limit options for cytotoxic T-lymphocyte escape in the immunodominant HLA-B27-restricted epitope in human immunodeficiency virus type 1 capsid. J. Virol. 82:5594–5605. http://dx.doi.org/10.1128/JVI.02356-07.
20. Brockman MA, Schneidewind A, Lahaie M, Schmidt A, Miura T, Desouza I, Ryvkin F, Derdeyn CA, Allen S, Hunter E, Mulenga J, Goepfert PA, Walker BD, Allen TM. 2007. Escape and compensation from early HLA-B57-mediated cytotoxic T-lymphocyte pressure on human immunodeficiency virus type 1 Gag alter capsid interactions with cyclophilin A. J. Virol. 81:12608–12618. http://dx.doi.org/10.1128/JVI.01369-07.
21. Valentine LE, Loffredo JT, Bean AT, Leon EJ, MacNair CE, Beal DR, Piaskowski SM, Klimentidis YC, Lank SM, Wiseman RW, Weinfurter JT, May GE, Rakasz EG, Wilson NA, Friedrich TC, O'Connor DH, Allison DB, Watkins DI. 2009. Infection with "escaped" virus variants impairs control of simian immunodeficiency virus SIVmac239 replication in Mamu-B*08-positive macaques. J. Virol. 83:11514–11527. http://dx.doi.org/10.1128/JVI.01298-09.